USING SYNTHETIC SKY-MAPS TO AID THE INTERPRETATION OF SZ-SURVEYS

Collaborators: G. Holder (McGill), P. Bode, J. Ostriker (Princeton), J. Weller, S. Bridle (UCL), A. Vale (Lisbon), Sadegh Kochfar (Oxford), Tom Crawford (Chicago)

Shaw et al. (07), accpted for pub in apj
Weller et al. (08), in prep

SUMMARY

1. Structure Formation and the Cosmological dependence of the mass function

2. Cluster mass estimation, scaling relations, sources of intrinsic scatter

3. Observatation/Systematic effects, cluster selection function

Mass distribution of halos

- CDM predicts hierarchical structure scheme:

    1. low mass perturbation collapse first
    2. merge to form more massive structures

- abundance of halos as a function of mass and redshift important quantity in cosmology

- Analytic predictions via Press-Schecter formalism (and subsequent variants) (Press & Schechter, 1974; Bond et al. 1992; Lacey & Cole 1994; Sheth & Tormen 1999; Jenkins et al. 2001)

    - smooth linear density field on range of mass scales
    - assume fraction of space contained within regions above some critical density, δ_c, is contained within collapsed objects

$$\frac{dn(M,z)}{dM} = -\sqrt{\frac{2}{\pi}}\frac{\rho_0}{M}\frac{\delta_c}{\sigma^2(M,z)}\frac{d\sigma(M,z)}{dM}\exp\left(-\frac{\delta_c^2}{2\sigma^2(M,z)}\right)$$

The N-body era

- Concerted effort over the last 15 years to simulation formation of structure and measure halo mass function [Cole & Lacey, 1993; Lacey & Cole, 1994; Governato et al. 1999; **Sheth & Tormen 1999**, Jenkins et al. 01; Springel et al. 05; Warren et al. 07)

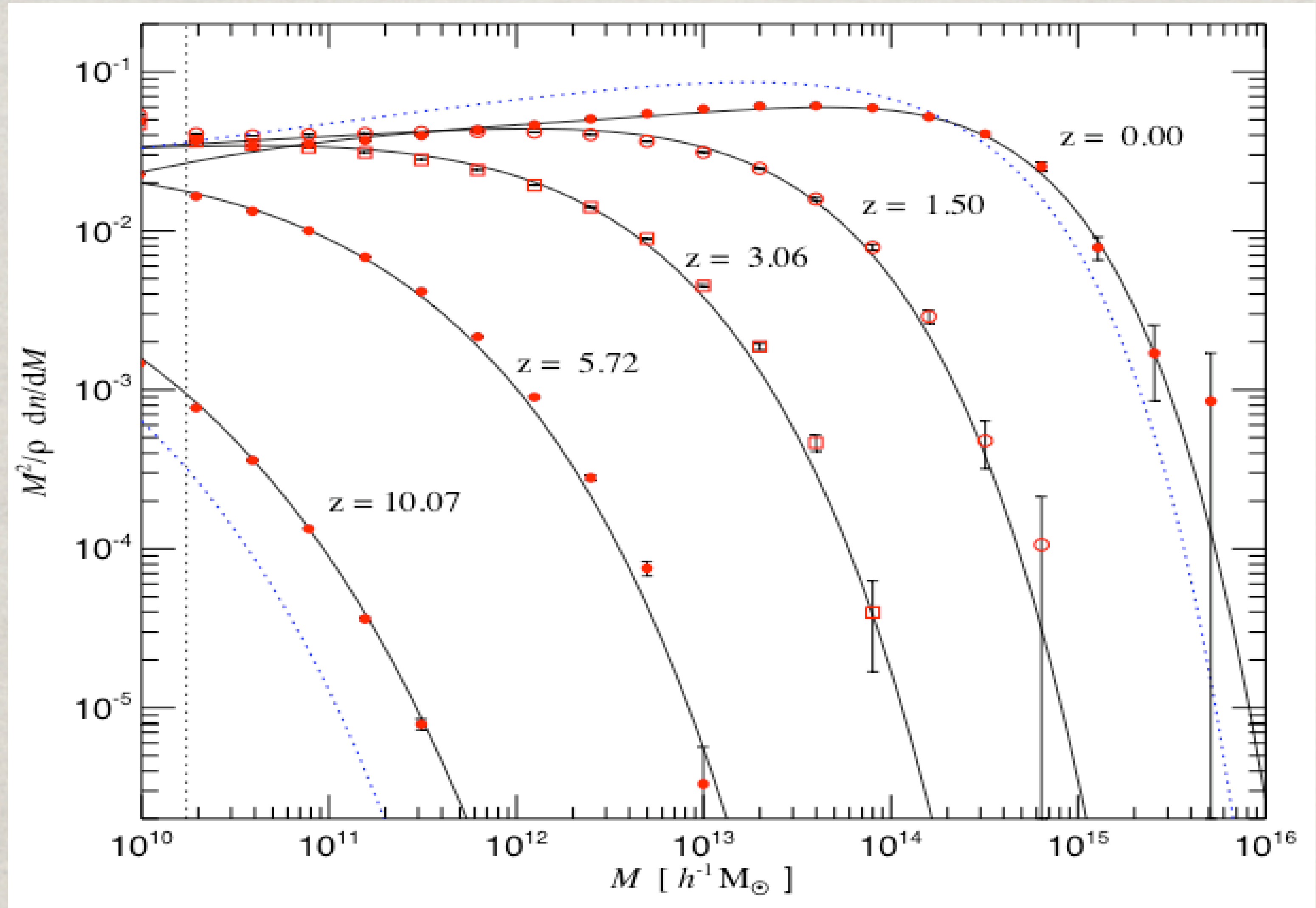

Springel et al. (2005)

- Jenkins et al. (01) demonstrated the <u>form</u> of the mass function is <u>independent* of epoch and cosmological parameters</u>

*in CDM, and depending on your definition of halo mass

Swedes armed with lightbulbs

Figure 1.7: Tidal deformations and the formation of spiral arms in the interacting galaxies (or 'nebulae') in the Holmberg 'lightbulb' experiment. *Upper* panel shows the results when galaxies initially rotate in a clockwise sense, and the *lower* panel for the anti-clockwise (*lower*) case. Figure taken from Holmberg (1941).

- C ... nation
  c ... 93;
  I ... Springel et
  a ...
  ... et al. (2005)
- Jenkins e ... nction
  is indepen

... definition of halo mass

The N-body era

- Concerted effort over the last 15 years to simulation formation of structure and measure halo mass function [Cole & Lacey, 1993; Lacey & Cole, 1994; Governato et al. 1999; **Sheth & Tormen 1999**, Jenkins et al. 01; Springel et al. 05; Warren et al. 07)

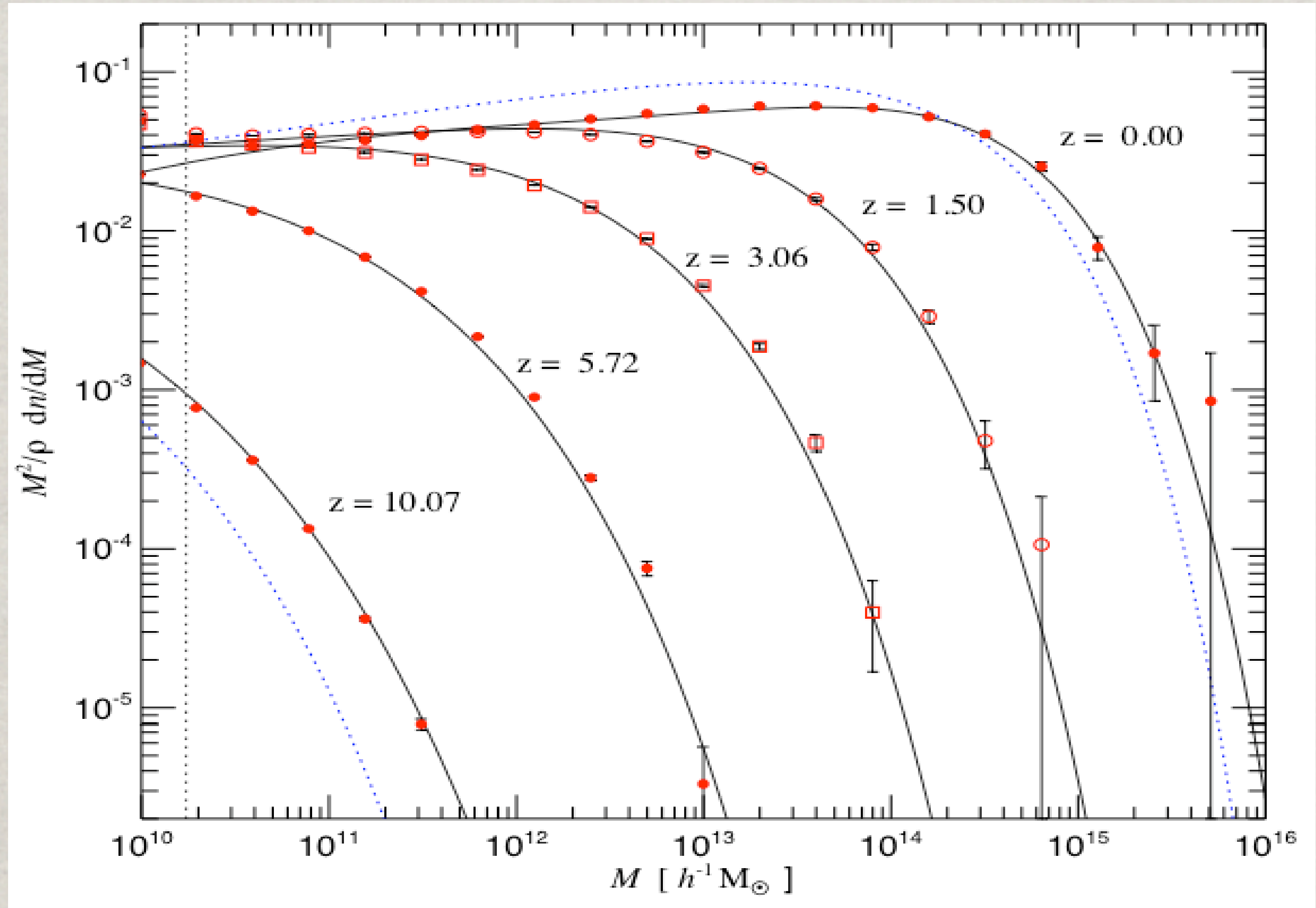

Springel et al. (2005)

- Jenkins et al. (01) demonstrated the form of the mass function is independent* of epoch and cosmological parameters

*in CDM, and depending on your definition of halo mass

Cosmological dependence

$$\frac{dn}{dM}(z, M) = -0.316 \frac{\rho_{m,0}}{M} \frac{d\sigma_M}{dM} \frac{1}{\sigma_M} \exp\left\{ - \left| 0.67 - \log[D(z)\sigma_M] \right|^{3.82} \right\}$$

- Mass density
- Power-law dependence on fluctuation amplitude
- Power-law dependence on linear growth factor

Cosmological dependence

$$\frac{dn}{dM}(z,M) = -0.316\frac{\rho_{m,0}}{M}\frac{d\sigma_M}{dM}\frac{1}{\sigma_M}\exp\left\{-\left|0.67-\log[D(z)\sigma_M]\right|^{3.82}\right\}$$

- $\boxed{\text{Mass density}}$
- Power-law dependence on fluctuation amplitude
- Power-law dependence on linear growth factor

Cosmological dependence

$$\frac{dn}{dM}(z,M) = -0.316\frac{\rho_{m,0}}{M}\frac{d\sigma_M}{dM}\frac{1}{\sigma_M}\exp\left\{-\left|0.67-\log[D(z)\sigma_M]\right|^{3.82}\right\}$$

- Mass density
- Power-law dependence on fluctuation amplitude
- Power-law dependence on linear growth factor

Cosmological dependence

$$\frac{dn}{dM}(z,M) = -0.316\frac{\rho_{m,0}}{M}\frac{d\sigma_M}{dM}\frac{1}{\sigma_M}\exp\left\{-\left|0.67-\log[D(z)\sigma_M]\right|^{3.82}\right\}$$

- Mass density
- Power-law dependence on fluctuation amplitude
- Power-law dependence on linear growth factor

Sky-surveys

$$\Delta N(z) = \Delta\Omega \int_{z-\Delta z/2}^{z+\Delta z/2} dz \frac{d^2V}{d\Omega dz} \int_{M_{\rm lim}}^{\infty} \frac{dn}{dM}\, dM$$

- Survey sky coverage
- Redshift bins
- Volume element
- Limiting mass of survey (redshift dependent)
- Cosmology dependence driven by volume element and mass function

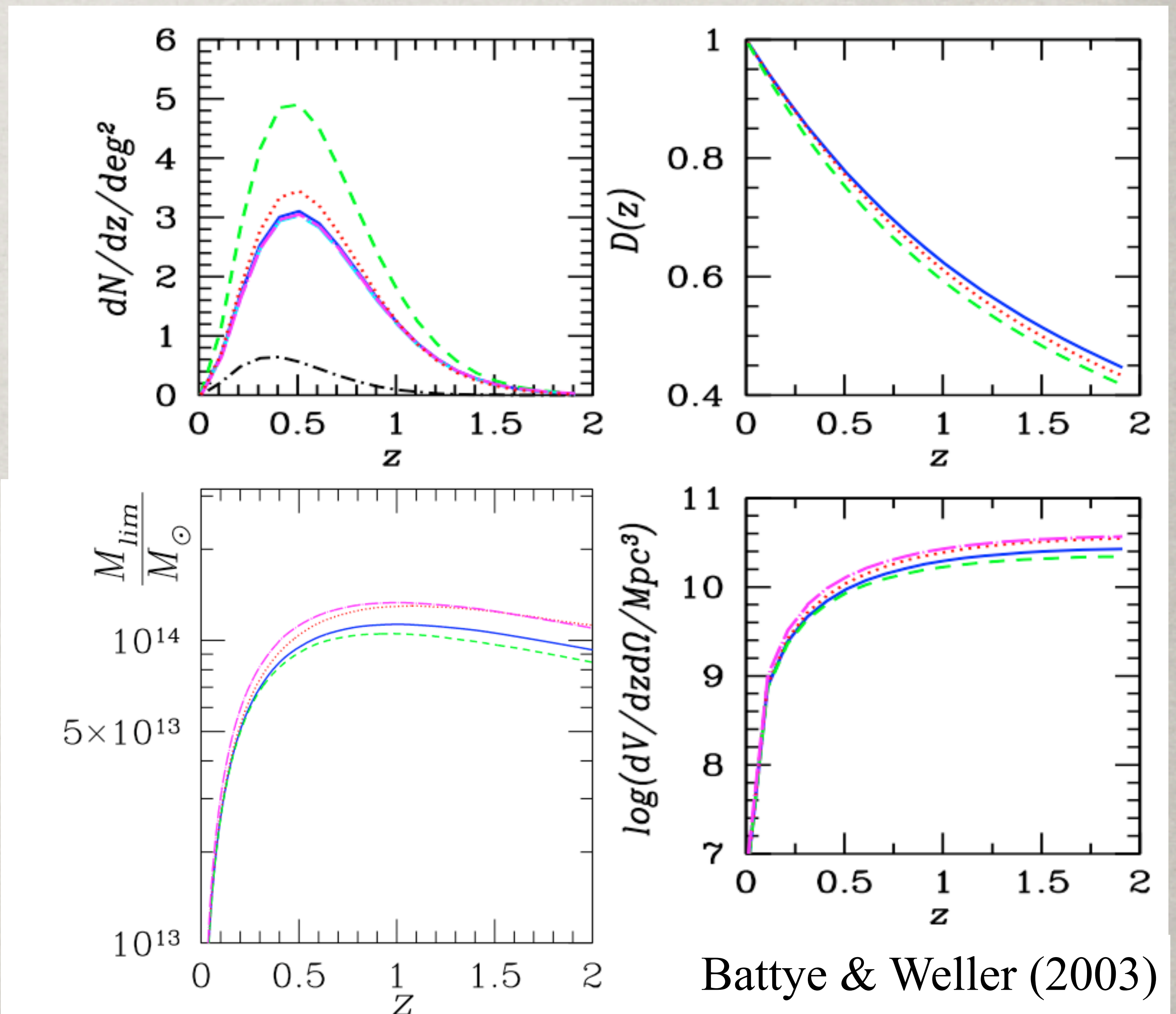

Battye & Weller (2003)

WEIGHING CLUSTERS

- Galaxies: Richness, velocity dispersion (see Gladders et al. 07, Koester et al. 07, Evrard et al. 08)
- Gas: X-ray luminosity/temperature/baryon fraction, SZ temperature decrement, (Motl et al. 05, Stanek et al. 06, Nagai 07, Morandi et al. 07, Schmidt & Allen 07, Rapetti et al. 08, many papers by Vikhlinin)
- Direct through lensing (strong/weak) aperture mass (Clowe et al. 2006, Bradac et al. 2006, Johnston et al. 2007)

Each proxy subject to different underlying physics and associated theoretical uncertainties.

Each provides probe of mass within **<u>different radii</u>**

DEFINING MASS

- normally defined as mass within region of spherical overdensity Δ times greater than critical density

$$M_\Delta = \frac{4}{3}\pi R_\Delta^3 \Delta \rho_c(z)$$

- spherical collapse model estimates overdensity of virialised (dynamically relaxed) halos

$$\beta \equiv \frac{2T_0 - E_s}{W_0} + 1 \, ,$$

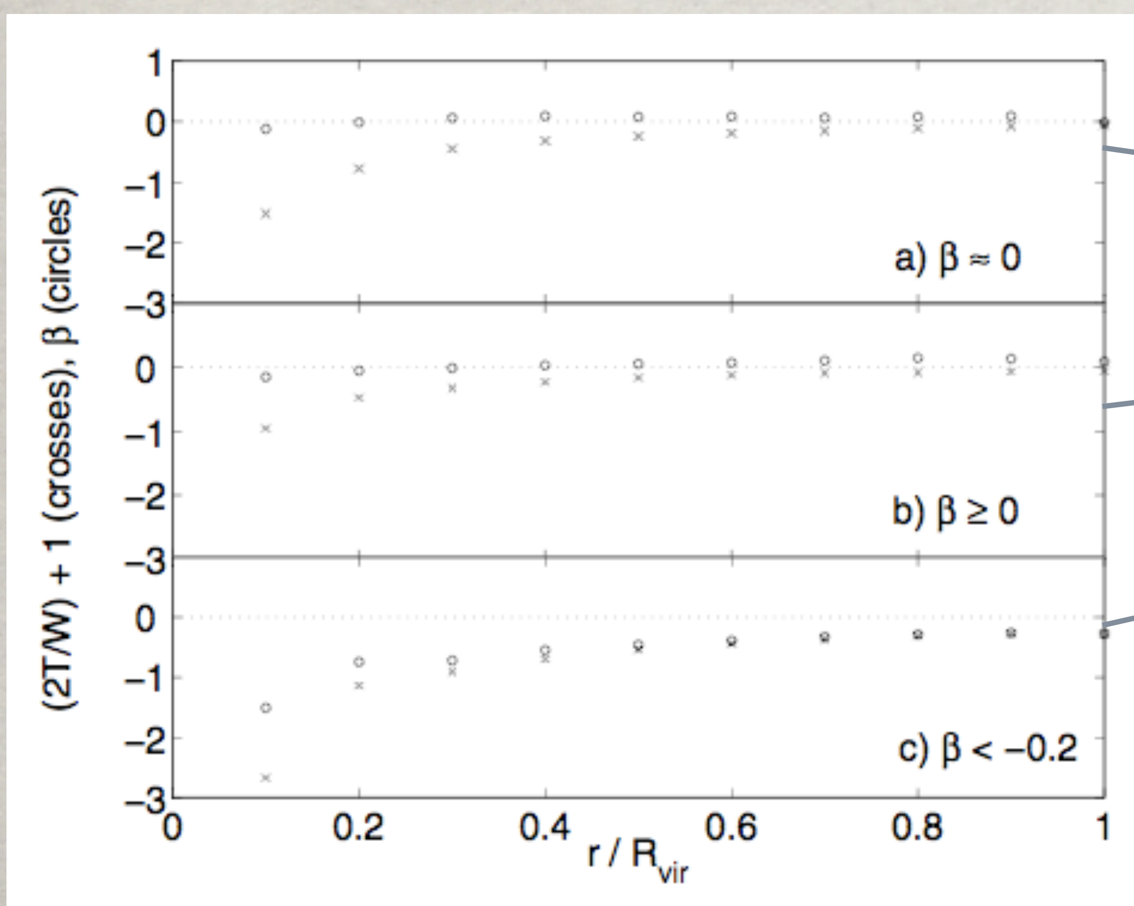

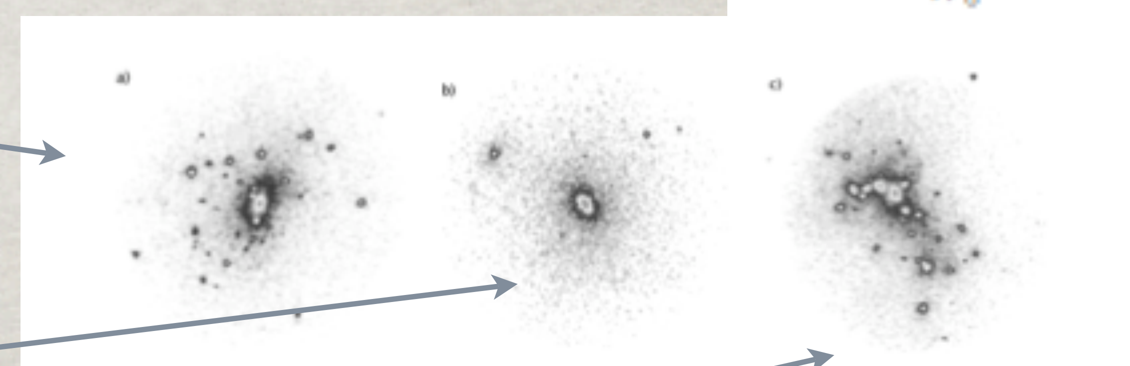

Fig. 3.— Projected density of the three example halos (labeled *a (top)*, *b (middle)* and *c (bottom)*) in Figure 2.

Shaw et al. (2006) [see also Cole and Lacey (96), Evrard et al (08)]

IMPACT OF SCATTER ON M.F.

- Scatter in M-obs relation causes clusters to scatter in to, and out of, sample
- steep slope of M.F. results in higher number of lower mass clusters scattering into sample, than those that scatter out

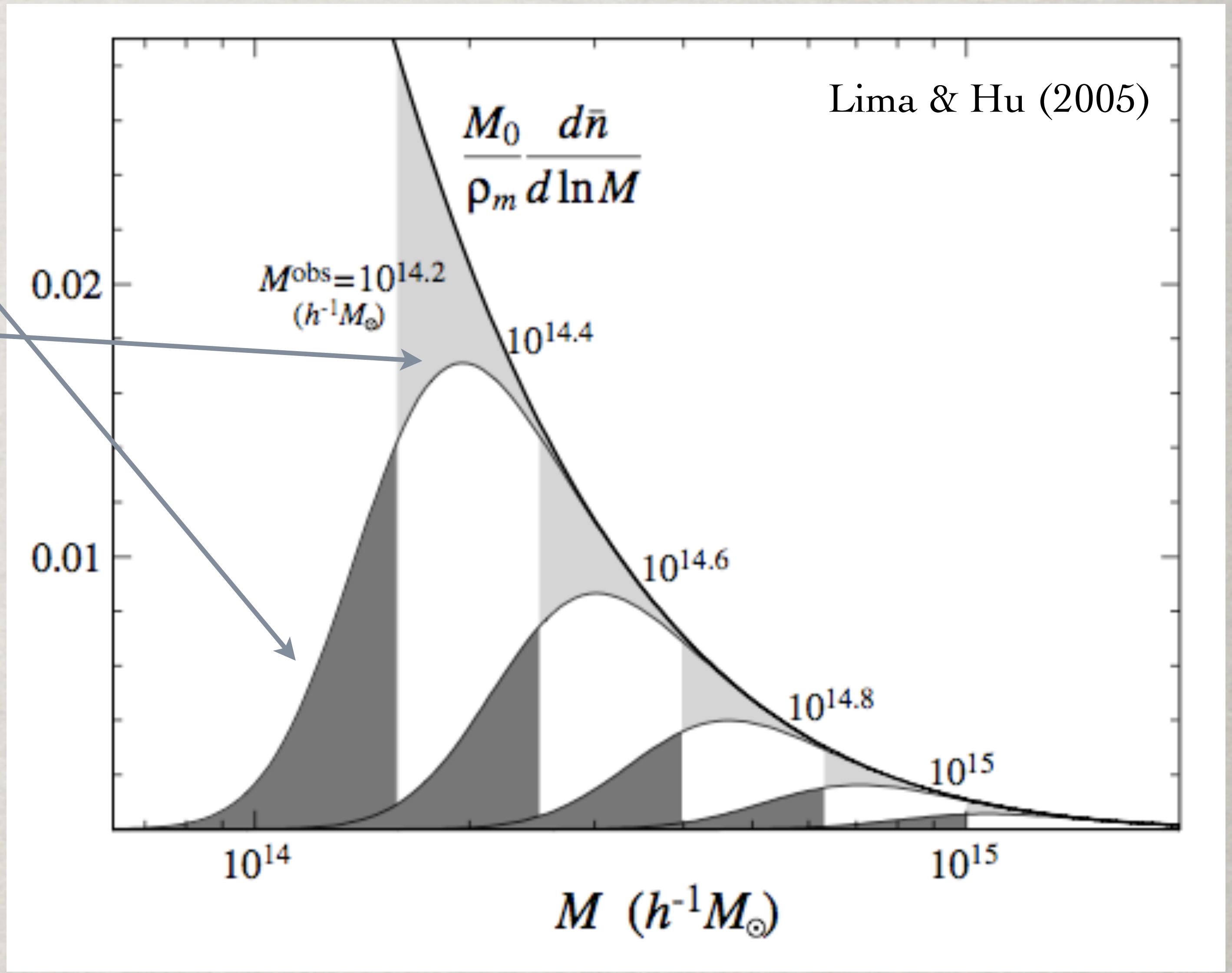

Important to have a handle on distribution of observed mass (e.g. Y, Lx, T, M_{lens}, B_{gc}) around true mass as a f(M,z)

IMPACT OF SCATTER ON M.F.

- Scatter in M-obs relation causes clusters to scatter in to, and out of, sample
- steep slope of M.F. results in higher number of lower mass clusters scattering into sample, than those that scatter out

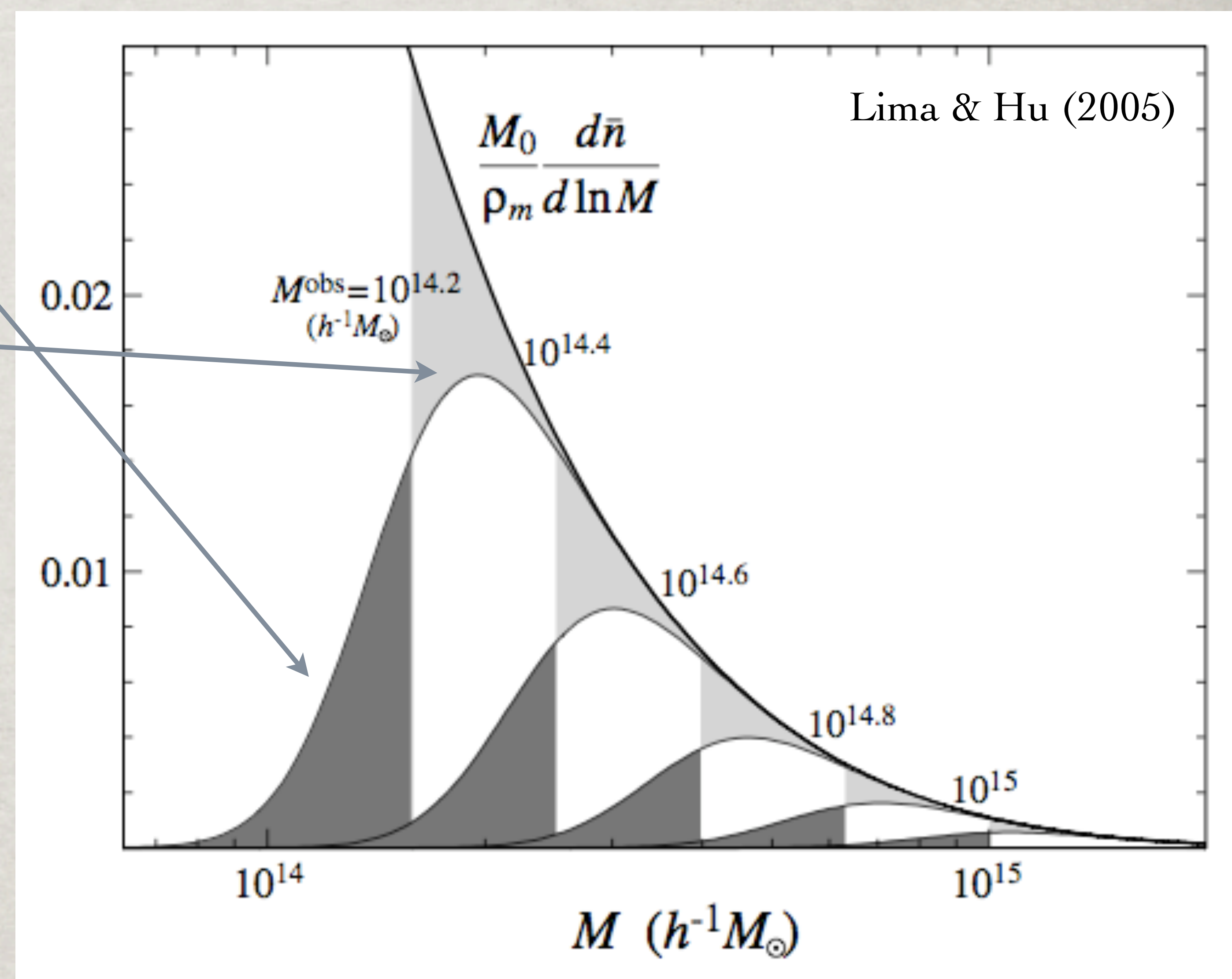

$$p(M_{obs}|M) = \frac{1}{\sqrt{2\pi\sigma^2_{\ln M}}} \exp\left[-x^2(M_{obs})\right]$$

$$x(M_{obs}) = \frac{\ln M_{obs} - \ln M - \ln M_{bias}}{\sigma_{\ln M}}$$

Important to have a handle on distribution of observed mass (e.g. Y, Lx, T, M_{lens}, B_{gc}) around true mass as a f(M,z)

Sunyaev-Zel'dovich Flux

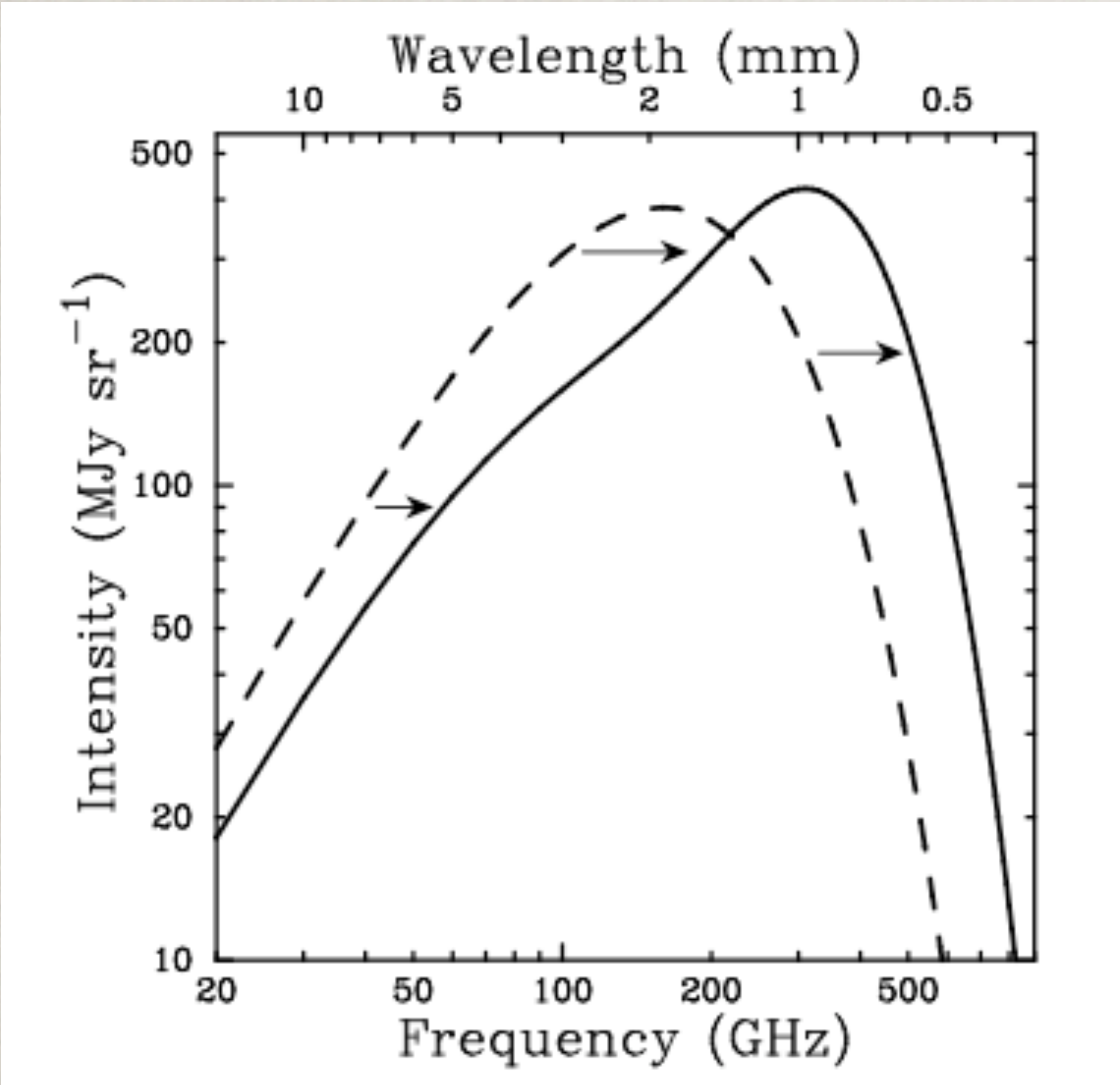

Carlstrom et al. 2002

- Inverse Compton Scattering:
  $e^- + \gamma \rightarrow e^- + \gamma$
- Surface brightness insensitive to redshift

$$\left(\frac{\Delta T}{T_{CMB}}\right)_{tsz} \equiv yY_0 = y(X coth(X/2) - 4)$$

$$y(\theta) = \frac{k_B \sigma_T}{m_e c^2} \int n_e T_e dl$$

For isothermal, spherically collapsed clusters in virial equilbrium (e.g. Battye & Weller, 03)

$$Y = \int_0^{\theta_{vir}} y(\theta) d\Omega \propto f_{gas} M_{vir}^{5/3} E(z)^{2/3}$$

Y-M scaling relations

- previous simulations typically find slopes of 1.66 (virial) to 1.9 depending on physics [c.f. White et al. (02), Motl et al (05), Nagai (06)]

- steeper slopes attributed to non-gravitational heating sources

- Scatter in relation found to be with in range 10-20% [c.f. Muanwong (02), da Silva (04), Nagai (06)]

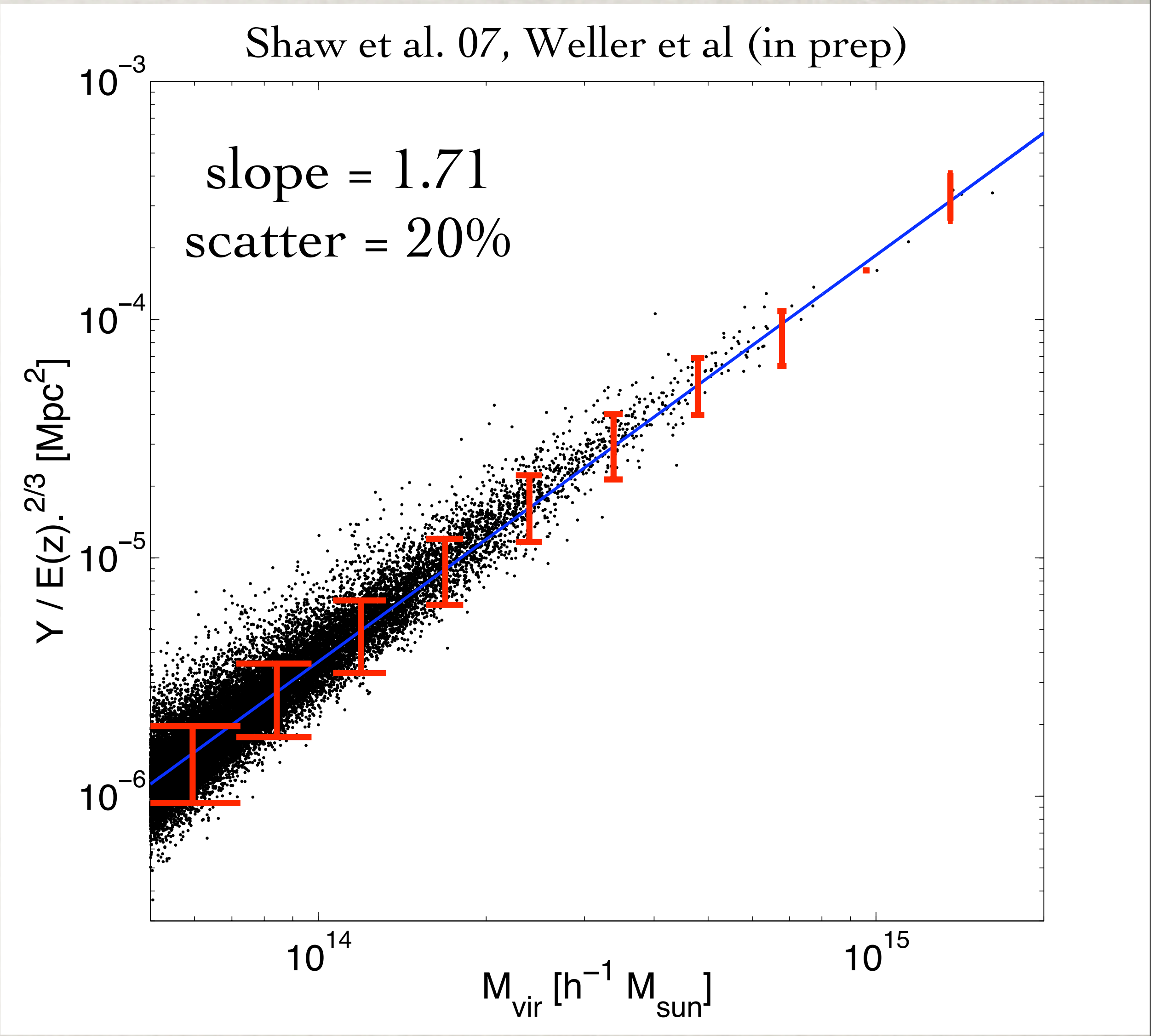

APEX, SPT, ACT

* Concerted effort to search for clusters via their SZ signature
* Surveys such as SPT, ACT
    - Image large areas of the sky (4000 deg^2)
    - multi-frequency (in range 90 - 220 GHz (90, 150, 220))
    - Noise levels down to 10's μK/1' pixel (10-30 μK)
    - Arc-minute beam size
* Optical follow-up for redshift -- Dark Energy Survey
    - 1 meter, 2.2 degree f.o.v., 500 megapixel camera on Blanco Telescope
    - 5000 sq. deg. (encompassing 4000 sq. deg. covered by SPT)
    - Photo-z (between $0.2 < z < 1.3$) for cluster redshift determination

Sources of Scatter and selection bias

- Intrinsic: variations between cluster properties

  - merger history (halo concentration & substructure)
  - morphology
  - baryonic/hydrodynamical processes (AGN activity, supernovae, shock heating, ram-pressure stripping)

Shaw et al. (07), Wik et al (08)

- Systematic/experimental:

  - large scale projection effects (SZ background) & primary CMB confusion
  - radio & sub-mm point sources
  - instrument noise, atmosphere
  - filtering

2×10^9 particles

Box side length
320 Mpc

TPM code
(Bode et al. 03)

$(\Omega_{\rm M}, \Omega_b, H_0, \sigma_8) =$
$(0.26, 0.044, 72, 0.77)$

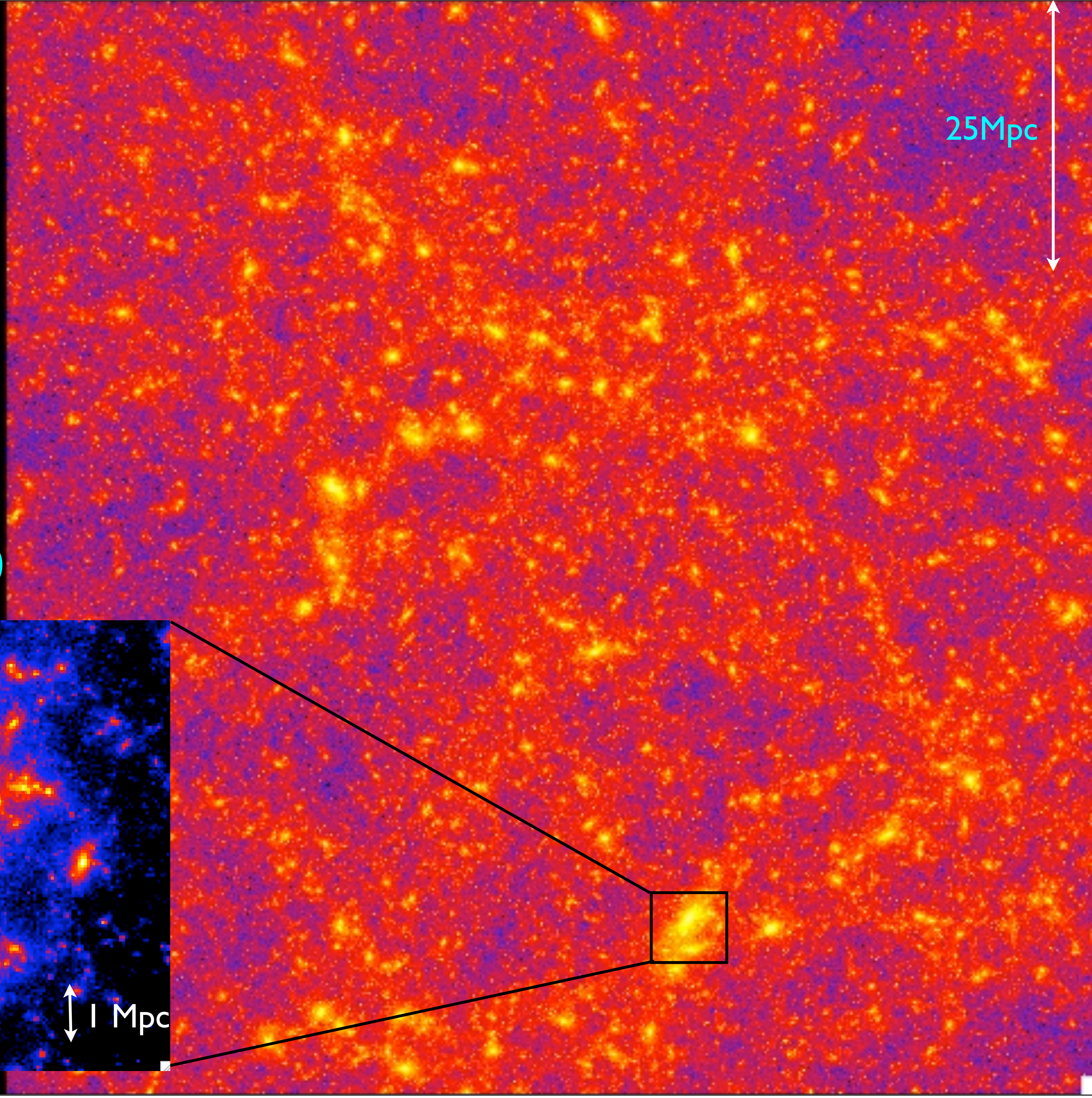

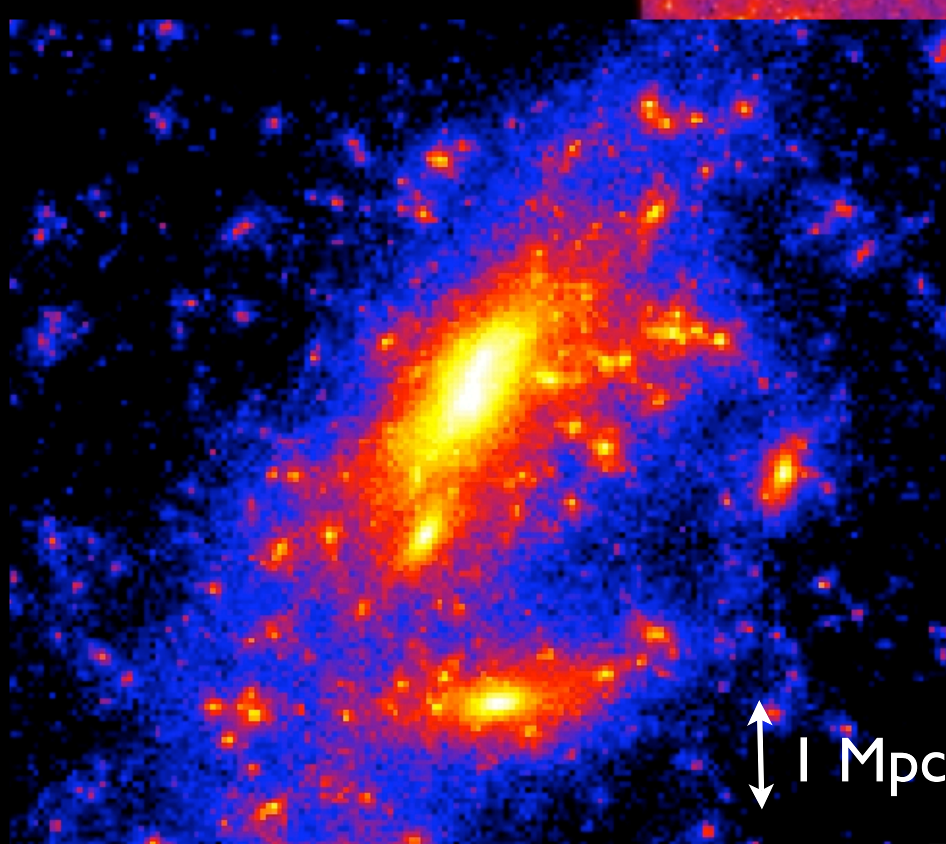

Intra-Cluster Gas model

- Gas model of Ostriker et al. (2005), Bode et al. (2007).
- Initial gas density/temperature determined from 3-d dark matter density/K.E, where $\rho_g = \rho_{dm}[\Omega_b/\Omega_M]$
- Rearrange gas assuming hydrostatic eq. + polytropic EoS (Γ = 1.2)
- Model Allows for: simple star formation prescription
  Feedback from SN & AGN, where
  $E_f = \epsilon_f M_* c^2$
- ϵ_f calibrated using using observed T-M, L_x-M, f_g-T relations

CALIBRATING FEEDBACK

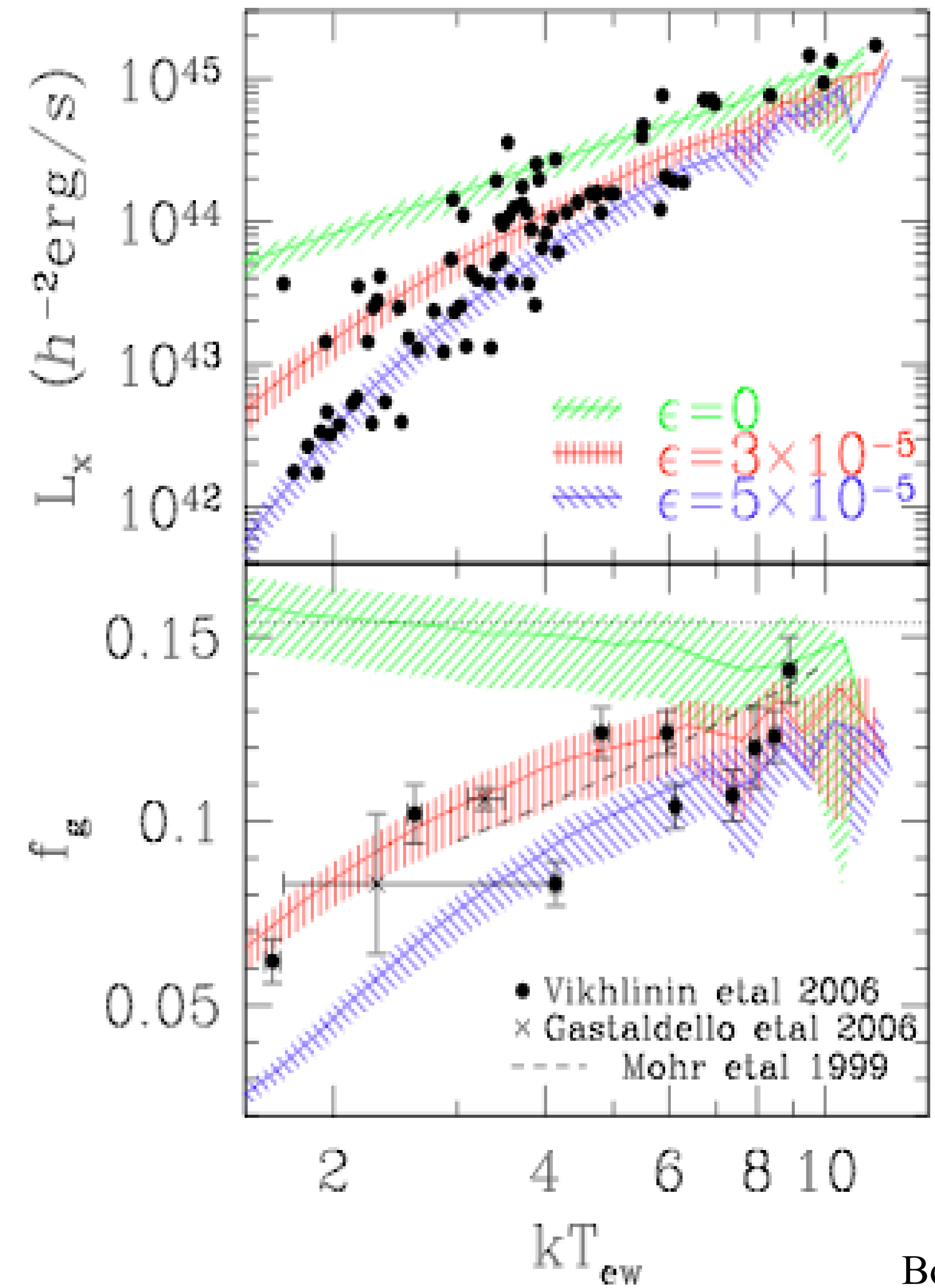

Bode et al. (2007)

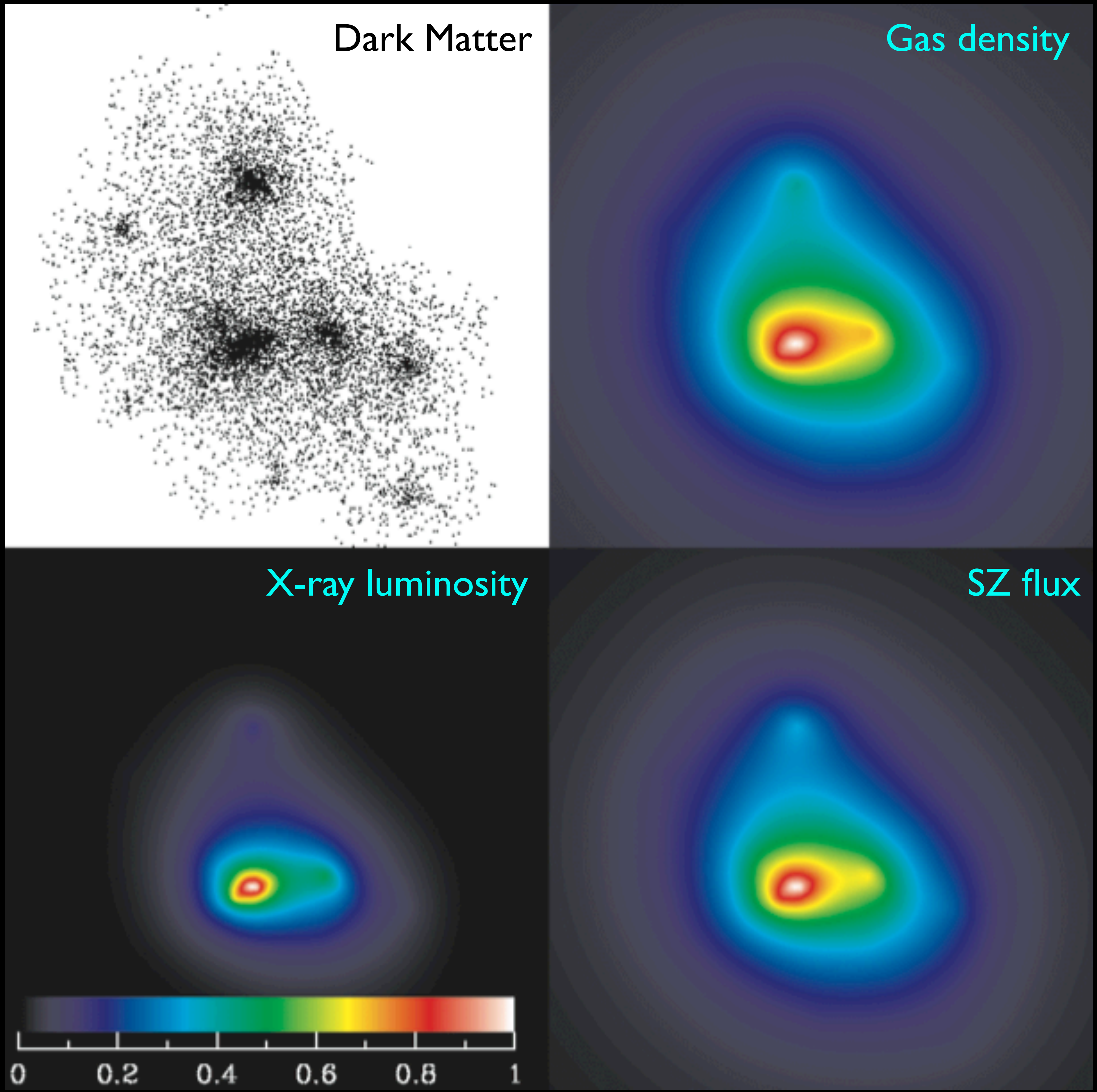
Dark Matter
Gas density
X-ray luminosity
SZ flux
0
0.2
0.4
0.6
0.8
1

Simulation samples

- N-body + ICM gas model allows generation of large cluster sample
  - 1267 clusters M_{sol} > 5 x 10^13 h^-1 M_{sol} (> 20,000 particles)
  - 2 realisations of gas model (ϵ_f = 4x10^-5, 0)
  - basic model, isothermal gas, rho_gas = f_b rho_dm
- Comparison sample extracted from adiabatic SPH (HYDRA) simulation [Muonwong et al. (02), Thomas et al. (02)]
  - 160^3 DM, 160^3 Gas
  - 212 clusters M_{sol} > 2.4 x 10^13 h^-1 M_{sol}

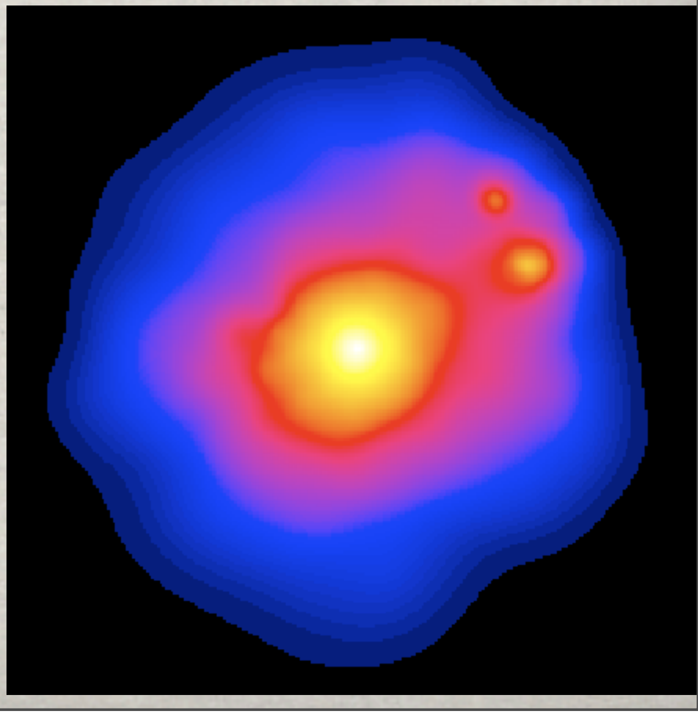

Definitions

- Can we define M and Y within some fiducial regions to empirically investigate tightest possible scaling?

- Measure Y_Δ and M_Δ within sequence of radii characterised by spherical overdensity $\Delta\rho_c$ in range $50 \le \Delta \le 1500$ $(0.37 \le r/R_{200} \le 1.77)$

- Plot all 256 combinations of Δ_Y and Δ_M

- Find best fit scaling

$$\hat{Y} = E(z)^{2/3} 10^A \left(\frac{M_\Delta}{10^{14} h^{-1} M_\odot} \right)^\alpha$$

- Define scatter

$$\sigma_{YM} = \left(\frac{\sum_{i=1}^{N} (\ln Y_{\Delta_Y} - \ln \hat{Y}_{\Delta_M})_i^2}{N-2} \right)^{1/2}$$

ENERGY FEEDBACK

gas model w/ fb — gas model, no fb

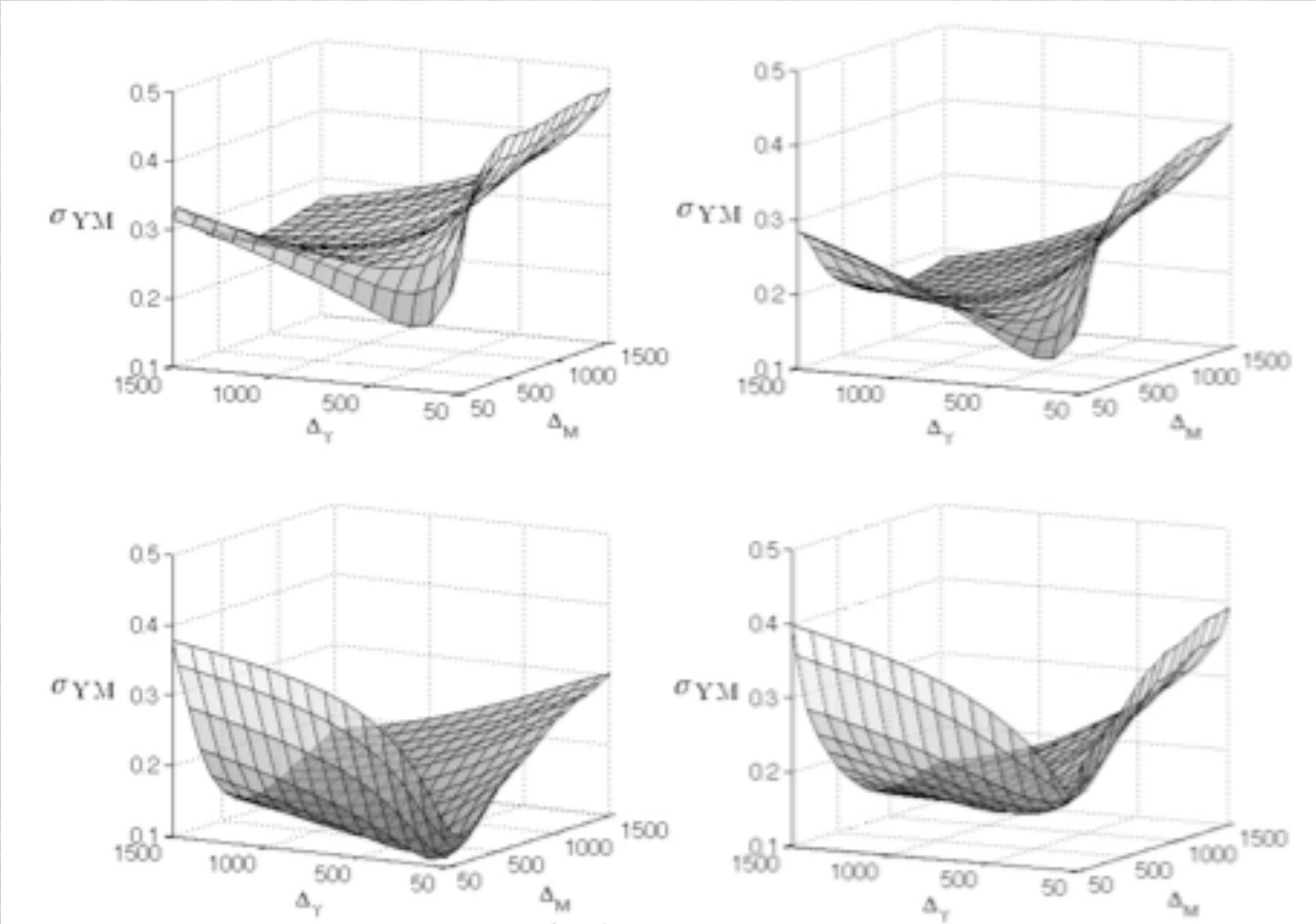

‘naive’ model — SPH

Substantial increase in scatter in ICM model incl. feedback due to greater variations in baryon fraction within R_Δ

HALO CONCENTRATION

- Halo concentration measures fraction of total halo mass contained in the inner regions

- Is thus probe of central potential -- energy scale of ICM

- Weak function of mass

- Wide distribution of c at any given mass

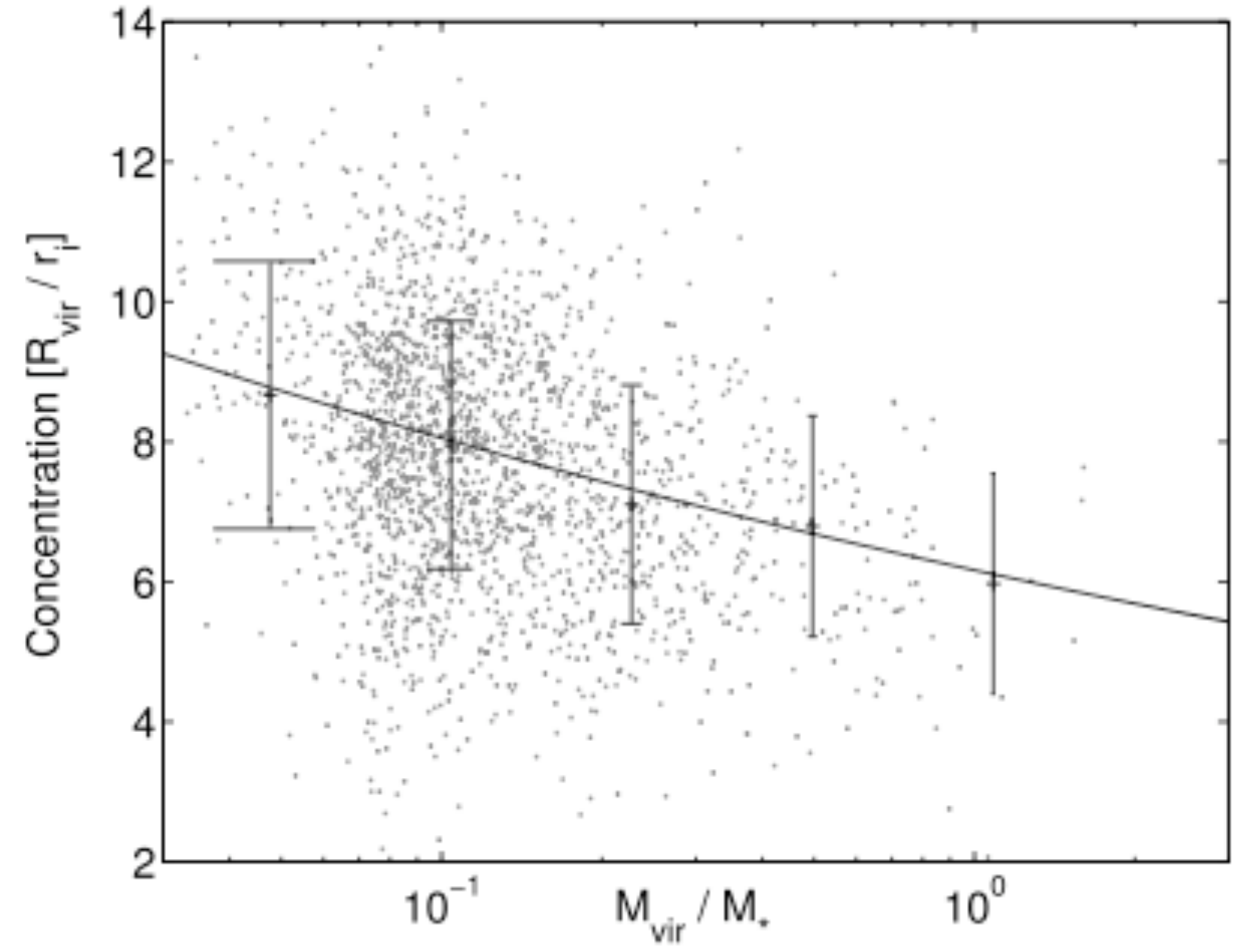

FIG. 20.—Scatter plot of concentration as a function of virial mass, having removed halos for which the NFW profile provides a poor fit due to large amounts of substructure. The points with error bars are the median concentration in logarithmic mass bins, the solid line is best fit of eq. (16) to the data ($\alpha = -0.12$ and $c_0 = 6.47$).

Shaw et al. (06)

IMPACT OF HALO STRUCTURE

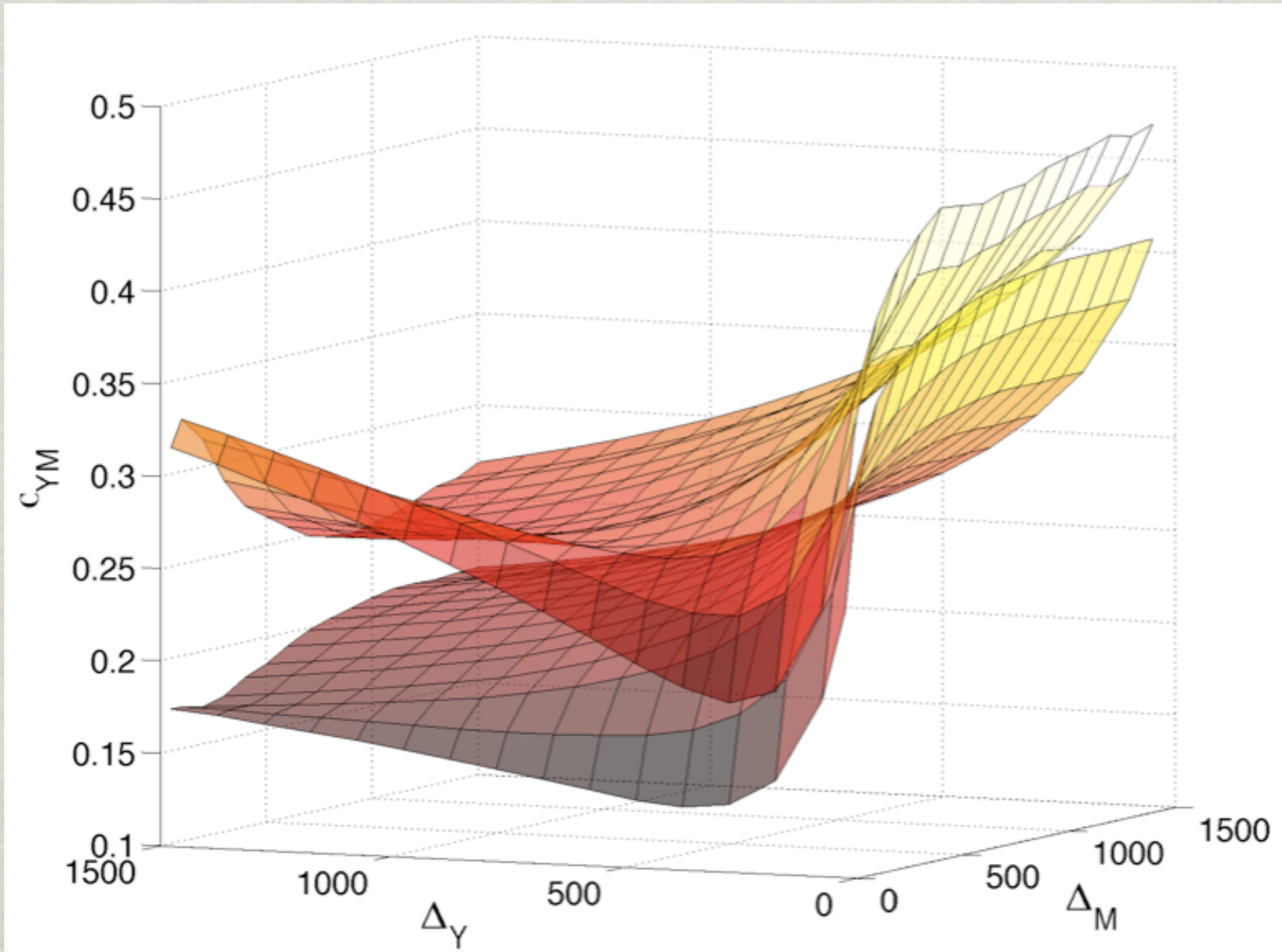

- constraining concentration by selection clusters that lie very close to *M*-c relation, reduces scatter by factor of 0.75 (contributes 5%)
[see also Reid and Spergel (06), Afshordi (07)]

central Decrement

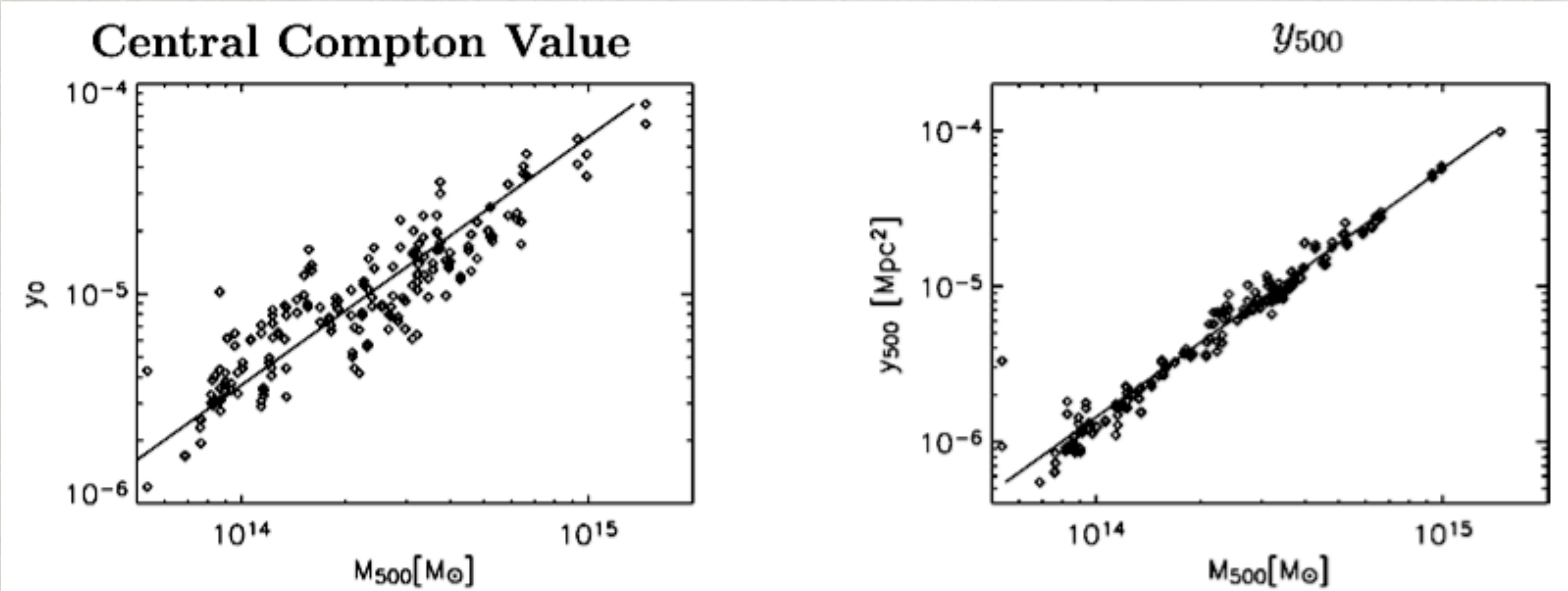

Motl et al. (05)

- Motl et al. (05) postulated that the central decrement is very sensitive to the dynamical state of the cluster, and is thus a poor proxy for mass
- Demonstrated by constraining variations in c at constant M

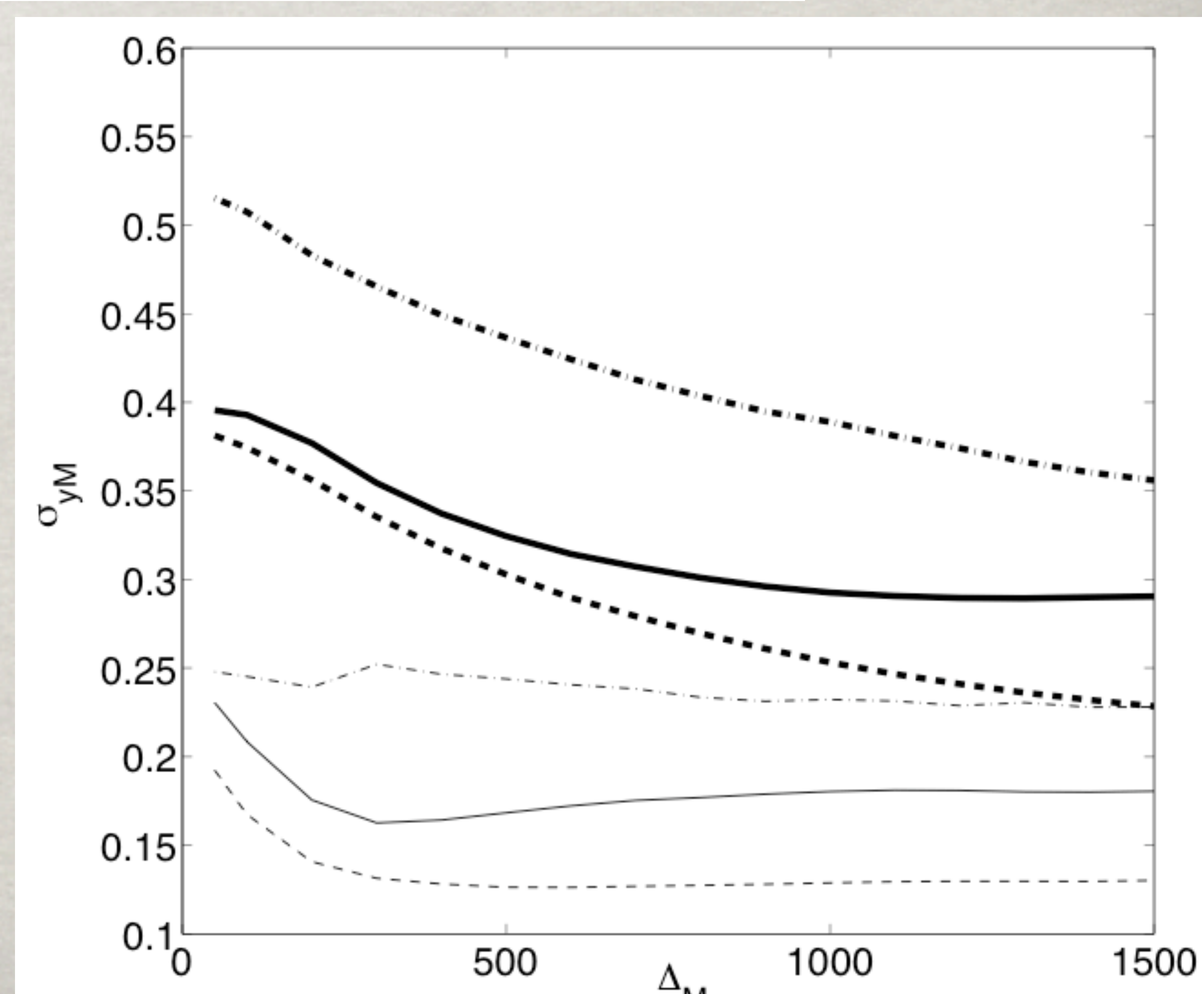

Shaw et al. (07)

CALIBRATING INTRINSIC SCATTER FROM SIMS

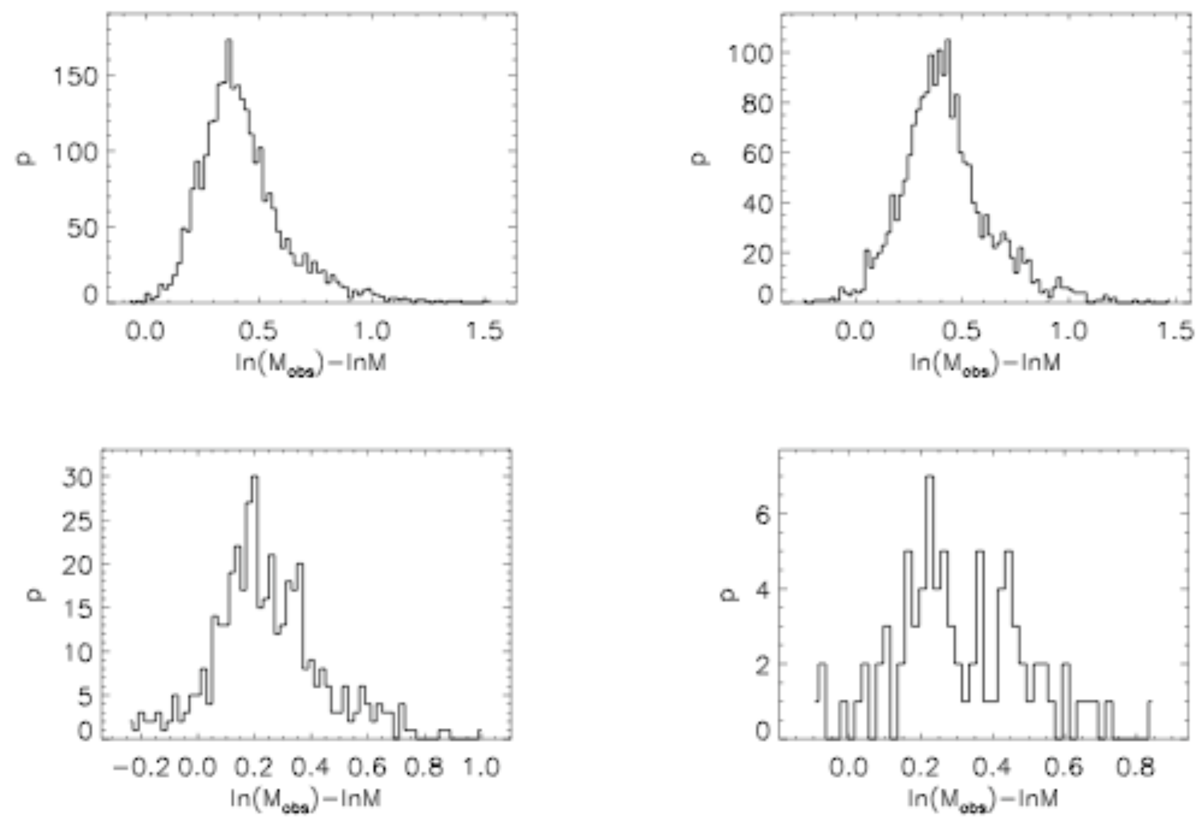

FIG. 14.— Distribution of the difference in 'observed' to true underlying mass. The mean is the bias or the normalization of the mass-observable relation. We assumed the measured slopes from Figure 13 for the conversion. Note that the normalization is arbitrary. The top left panel is for $z = 0.1 - 0.2$ and we obtain $\ln M^{\rm bias} = 0.44$ and $\sigma_{\ln M} = 0.19$, the top right panel is for $z = 0.5 - 0.6$ with $\ln M^{\rm bias} = 0.43$ and $\sigma_{\ln M} = 0.21$, the lower left panel for $z = 1.0 - 1.1$ with $\ln M^{\rm bias} = 0.25$ and $\sigma_{\ln M} = 0.19$ and the lower right one for $z = 1.4 - 1.5$ with $\ln M^{\rm bias} = 0.32$ and $\sigma_{\ln M} = 0.19$.

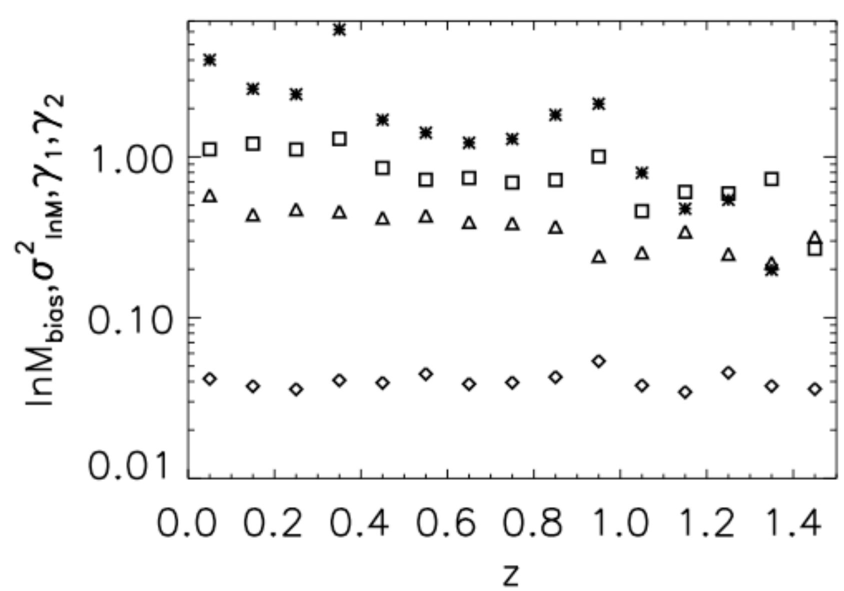

FIG. 15.— Statistical coefficients of the distribution of the mass - observable relation in different redshift bins. The mean (or bias) $\ln M^{\rm bias}$ as triangles, the variance $\sigma^2_{\ln M}$ as diamonds, the skewness as squares and the kurtosis as asterisks.

Weller et al (in prep.)

- Is intrinsic scatter normally distributed?
- If not, how do higher moments effect M.F.?

SYSTEMATIC & EXPERIMENTAL

- Intrinsic: variations between cluster properties
    - host dark matter halo concentration,
    - merger history (substructure)
    - morphology
    - baryonic/hydrodynamical processes (AGN activity, supernovae, shock heating, ram-pressure stripping)
- Systematic/experimental:
    - large scale projection effects (SZ background) & primary CMB confusion
    - radio & sub-mm point sources
    - instrument noise, uneven coverage, atmosphere
    - filtering

Map-making

N-body simulations

lightcone construction

Identify halos (FoF)

semi-analytic model for gas

ray trace through LC

add noise (CMB, instrument, point sources, SZ bg)

- N-body + semi-analytic gas model
- Enables runs with large box size -> larger field of view with less box repetition
- Can be re-run faster than hydro codes -> 'simulation' libraries mapping out cosmological parameter space.

Lightcone

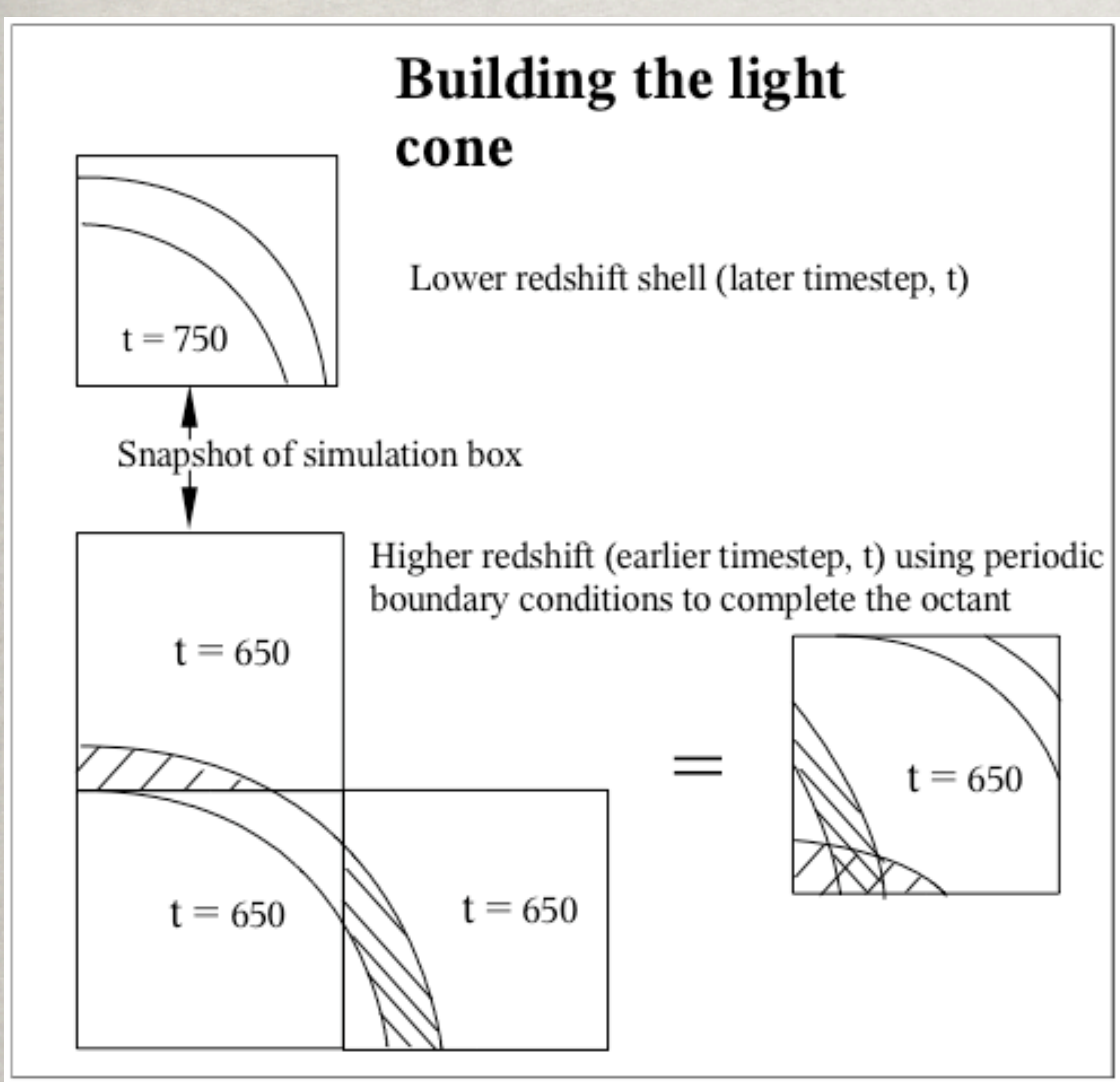

- chart matter distribution saved using 190 simulation outputs from z = 0-1.5
- total angular size = octant (~5250 deg^2)
- >2 million halos total above 10^{13} h^{-1} M_{sol}
- complete > 3×10^{13} h^{-1} M_{sol}

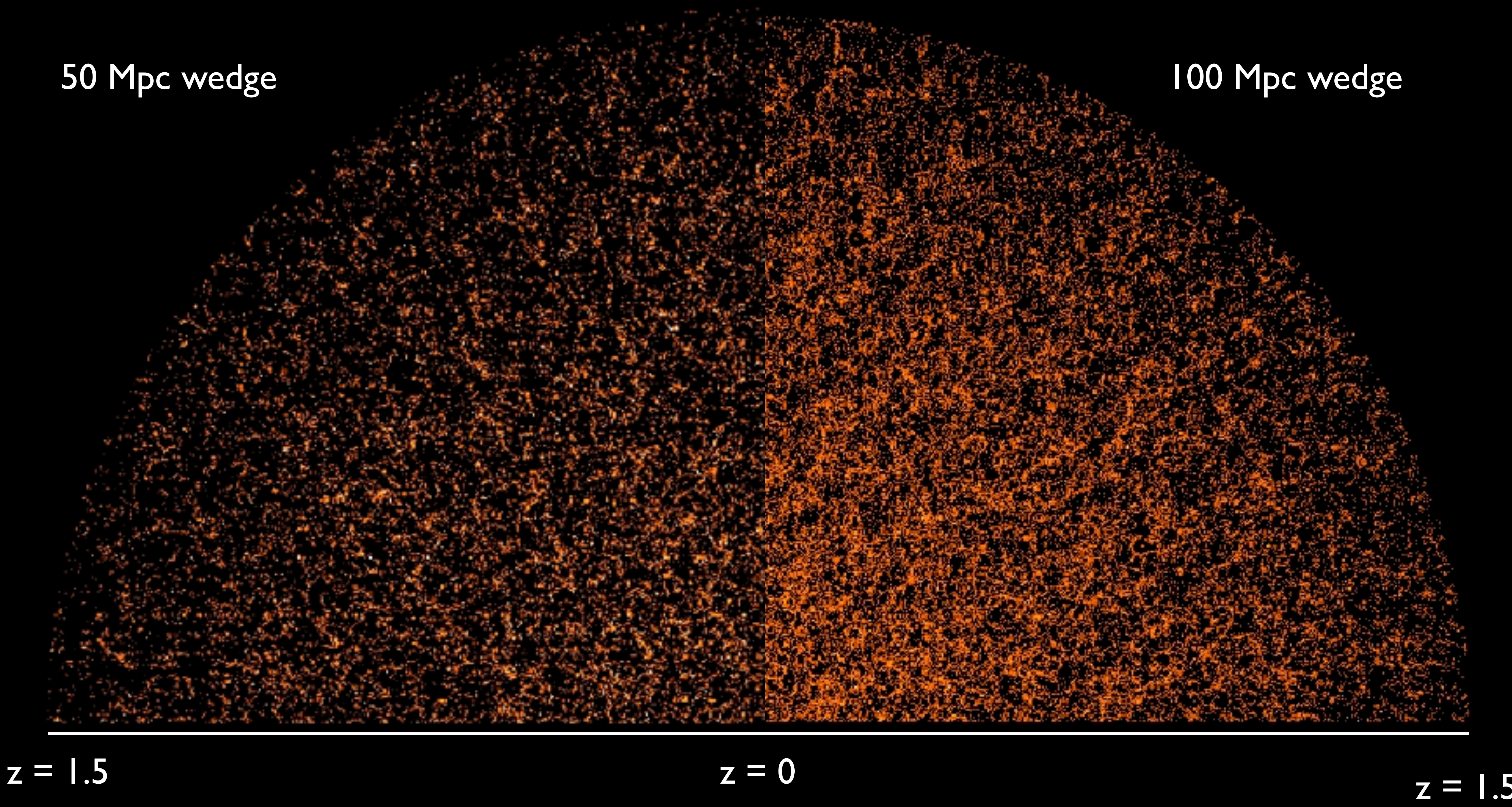
50 Mpc wedge
100 Mpc wedge
z = 1.5
z = 0
z = 1.5

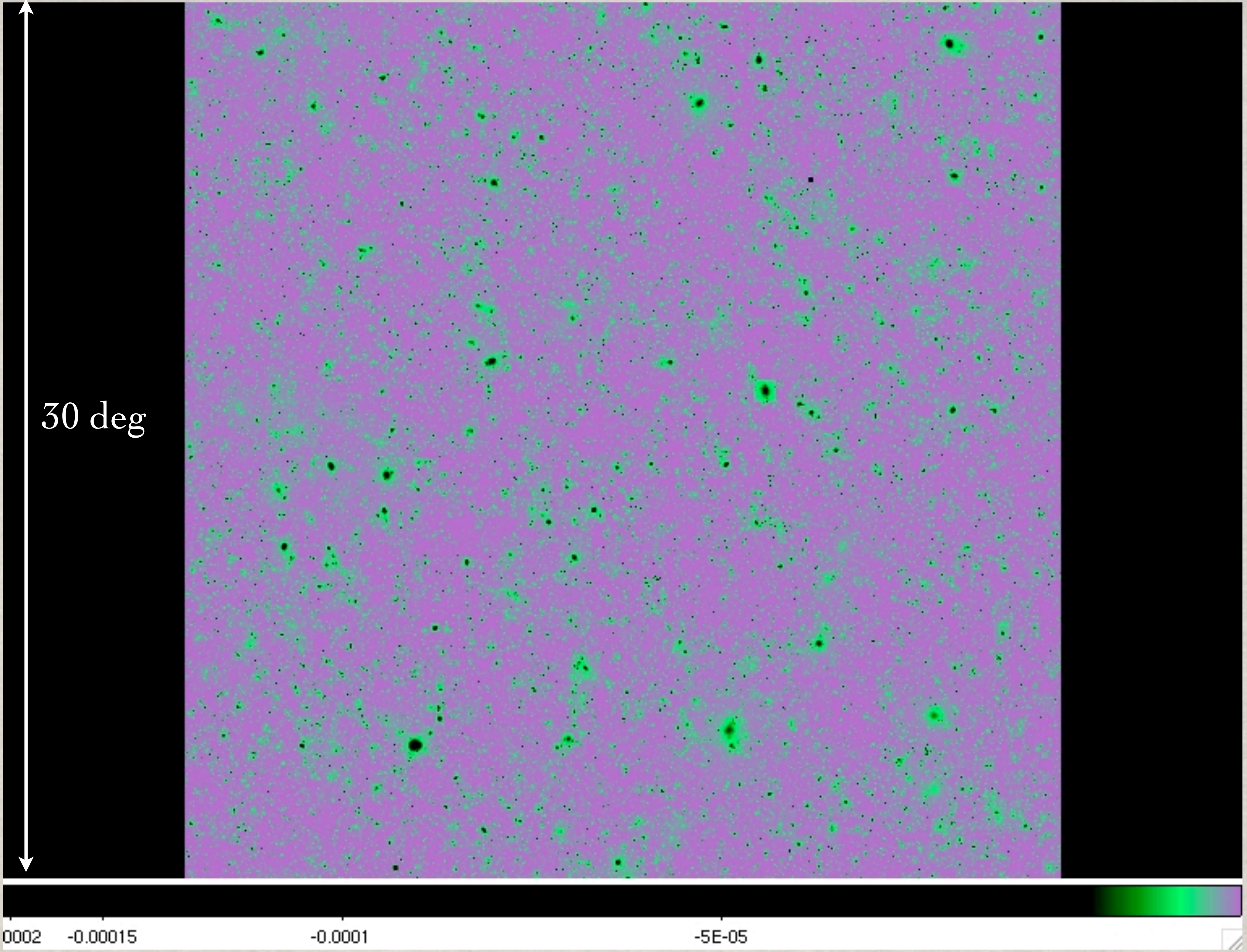
30 deg
0002
-0.00015
-0.0001
-5E-05

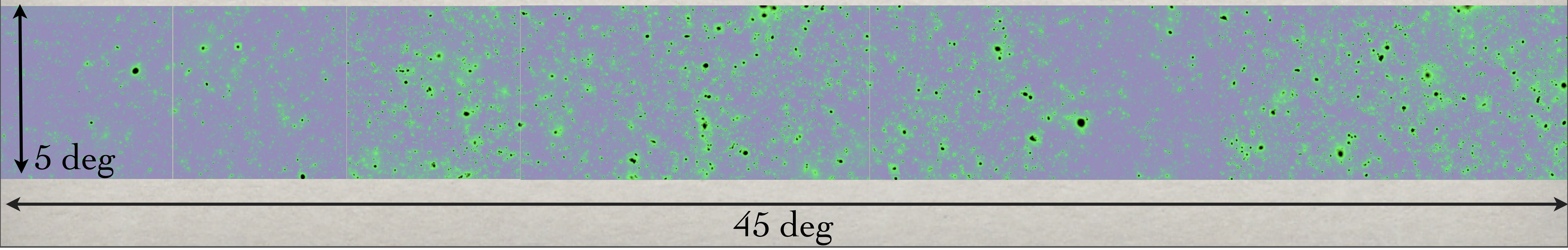
5 deg
45 deg

IMPACT OF SZ BACKGROUND

- confusion due to low-mass unresolved structure along line of sight [White et al. 2002, Holder et al. 07, Hallman et al. 07]
- Y is a <u>projected</u> quantity, so all gas along LoS contributes
- significant source of scatter in Y_{obs} - M

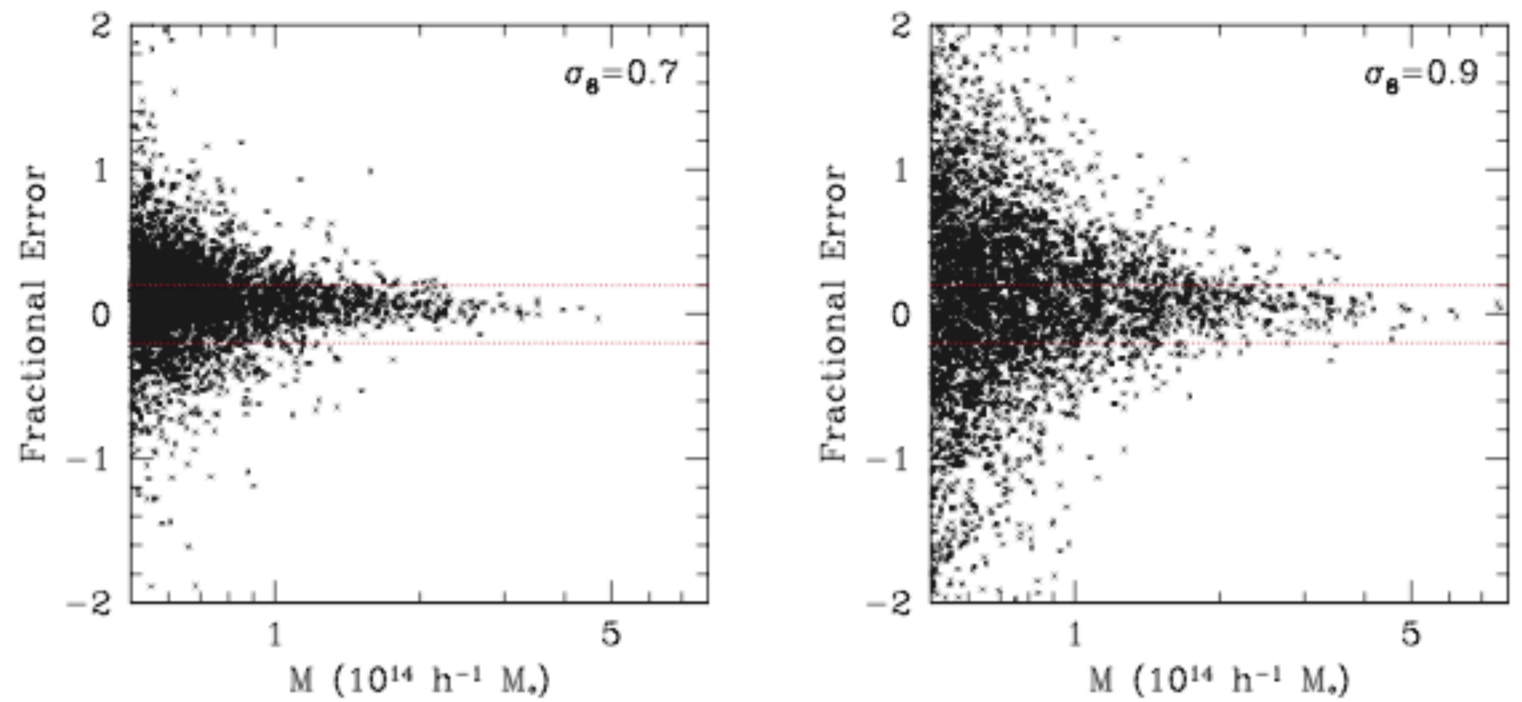

Figure 6. Fractional error in the SZ flux [calculated as (map-model)/model] in the $2^\circ \times 2^\circ$ filtered sky maps at the projected position of the input haloes in all 100 realizations of the $S_\circ = 200, \sigma_8 = 0.9$ (right-hand panel) and $\sigma_8 = 0.7$ (left-hand panel) model. The dotted lines show ±20 per cent errors. Each panel shows 10 000 clusters selected randomly from the ensemble of maps.

Holder et al (07)

- provides lower limit to the mass of clusters that can be reliably measured

SZ Background on M-Y

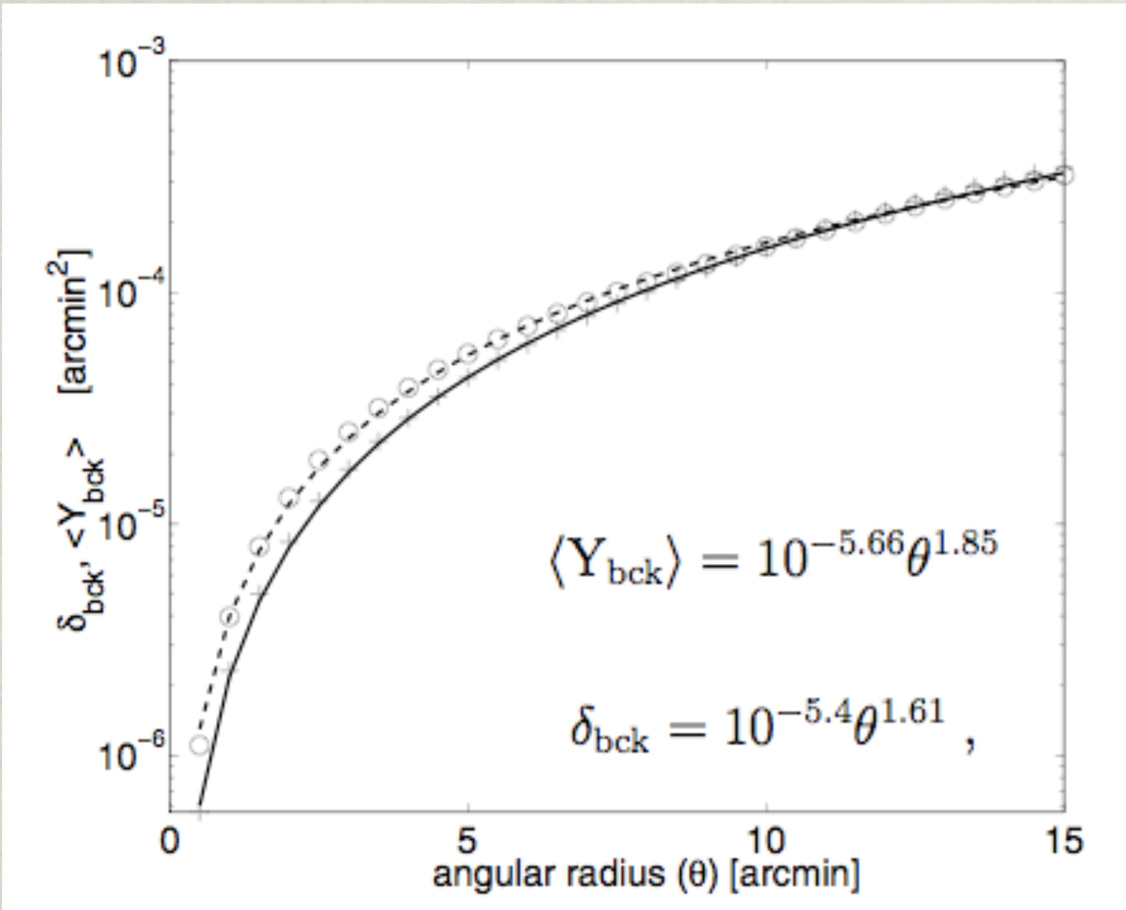

- Using lightcone clusters to evaluate mean background flux $<Y_{bck}>$ and variance δ_{bck}^2

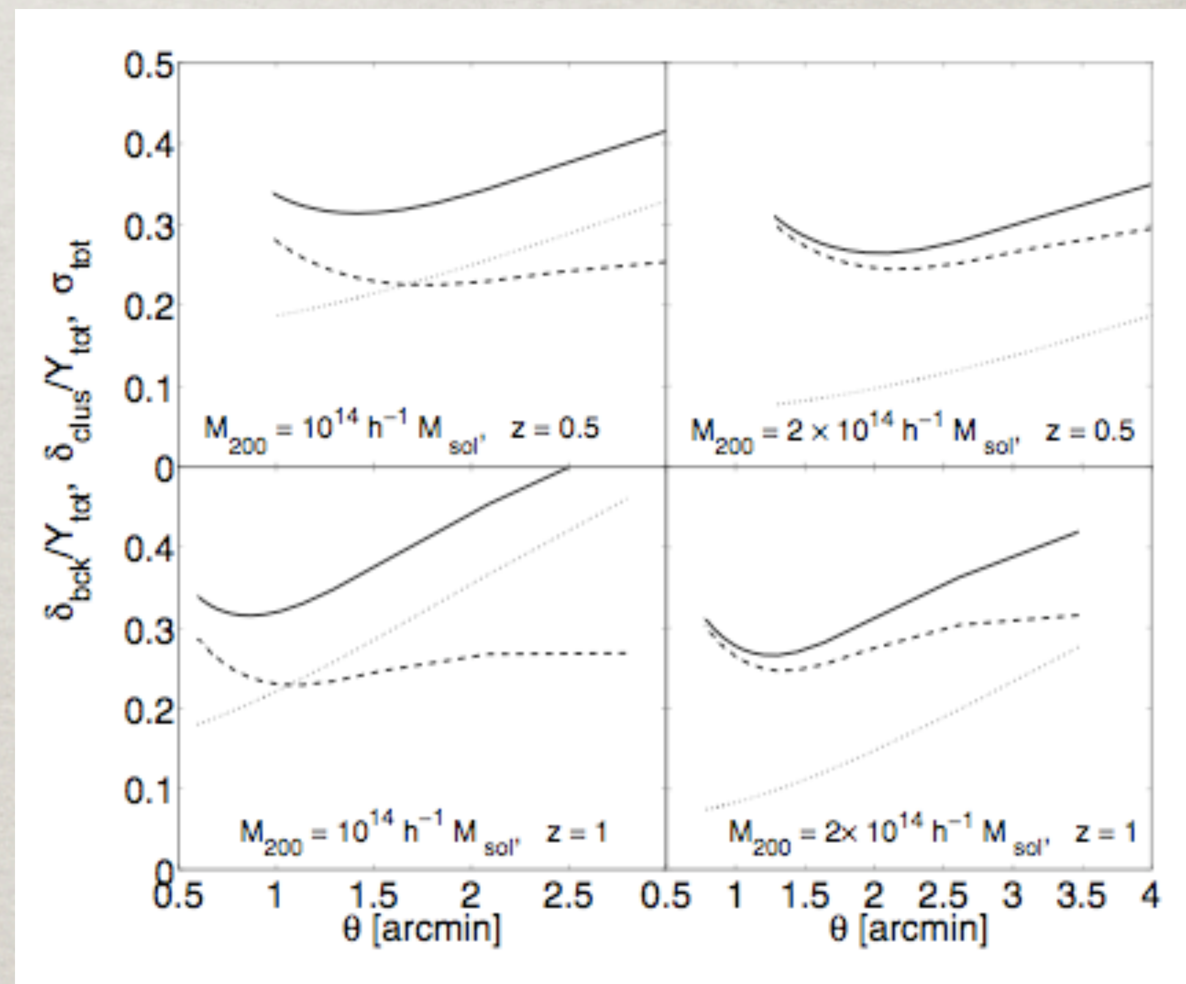

- combine intrinsic scatter with that due to SZ bg. (using $\Delta_M = 200$)

- determine optimal angular radius

$$\sigma_{tot}(\theta, M, z) = \frac{(\delta^2_{bck(\theta)} + \delta^2_{clus})^{\frac{1}{2}}}{Y_{\rm tot}}$$

Optimal angular Aperture

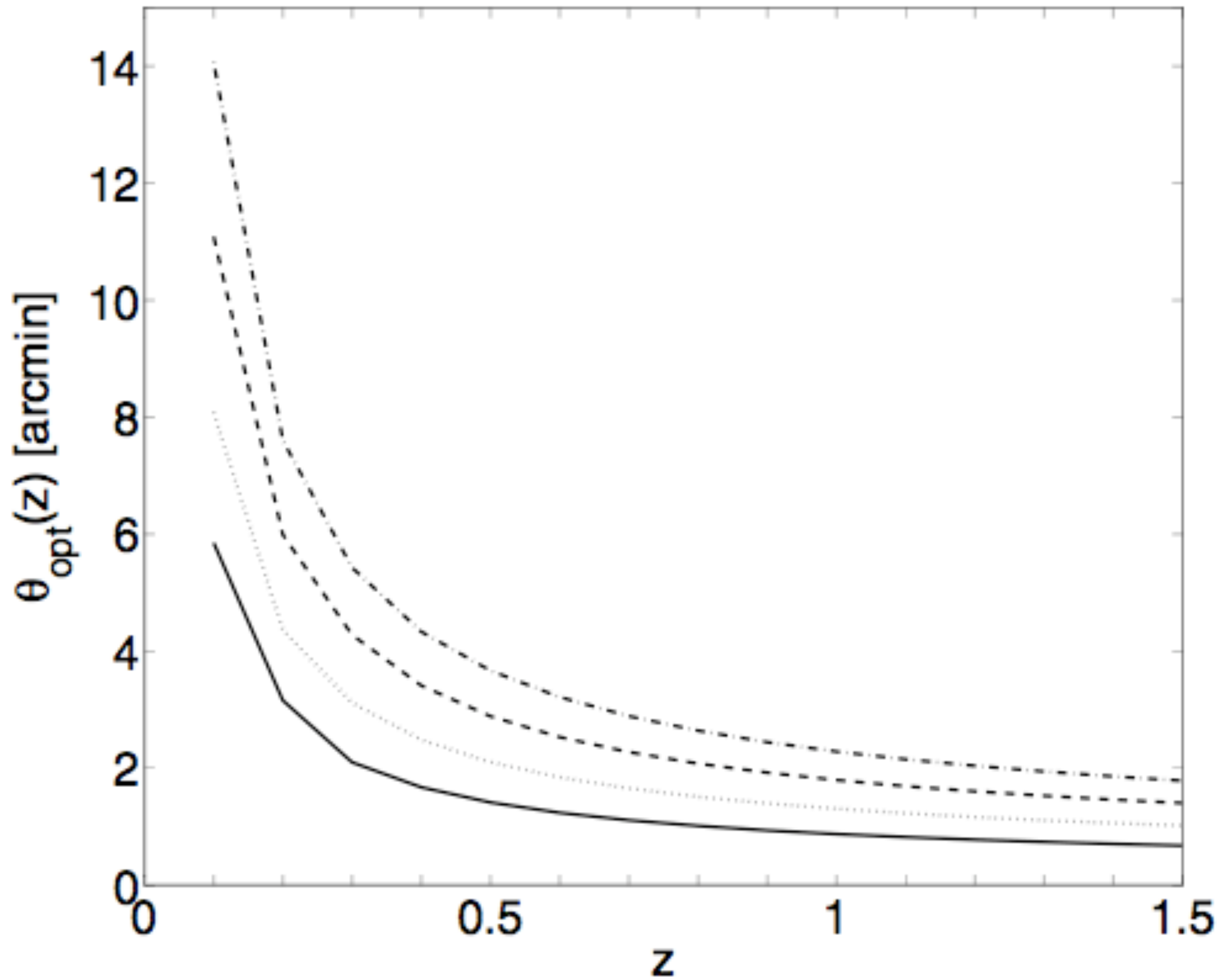

Fig. 8.— The optimal angle θ_{opt} within which SZE flux can be measured for a cluster of mass 10^{14} (*solid line*), 2×10^{14} (*dotted*), 5×10^{14} (*dashed*) and 10^{15} (*dot-dashed*) $h^{-1}M_{\odot}$ to give the least scatter (intrinsic plus projected) in the $Y - M$ relation cluster at redshift z.

results appear largely insensitive to gas physics, but will be strong dependent on σ_8. Point sources also a big problem

Noise

- ✓ Primary CMB (flat-sky)
- ✓ SZ background
- ✓ Instrument noise (isotropic)
- ✓ Sub-mm sources

To Add:

- ✦ radio point sources?
- ✦ non-isotropic inst. noise?

generate library of
noise map (and point source
catalogues) corresponding
to sections of simulation sky

Sub-mm sources

- Following Knox et al. (04)....
- Monte carlo catalogue at 350GHz, using flux distribution from SCUBA observations (Borys et al. (03)

$$\frac{dN(>S)}{dS} = \frac{N_0}{S_0}\left[\left(\frac{S}{S_0}\right)^{\alpha} + \left(\frac{S}{S_0}\right)^{\beta}\right]^{-1}$$

- convert flux between frequencies assuming spectral index α = 2.6 +- 0.3

$$S_\nu = S_{150}\left(\frac{\nu}{150\,\mathrm{Ghz}}\right)^{\alpha}$$

- Lower limit of 2mJy at 350Ghz

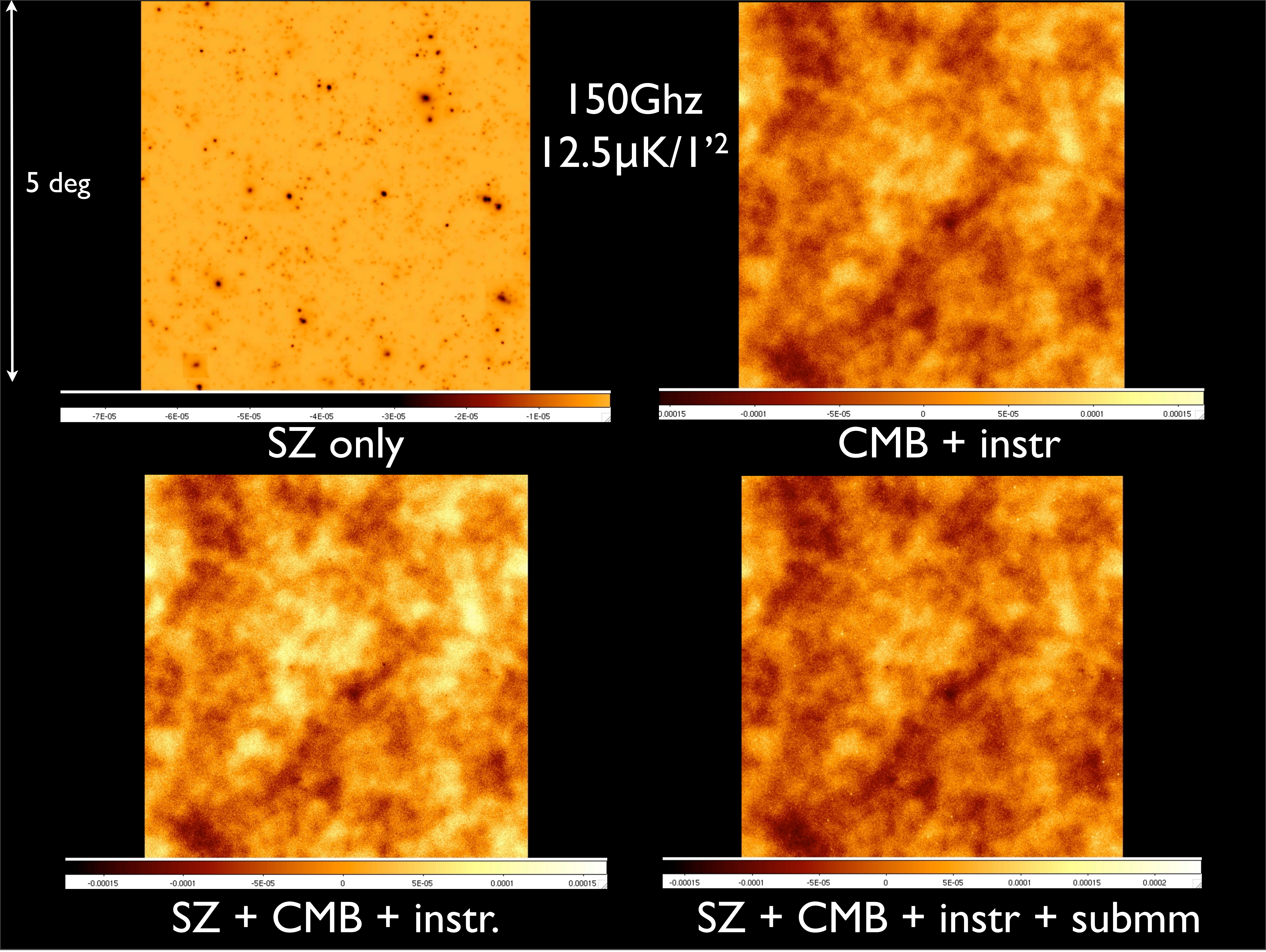
150Ghz
12.5μK/1'2
5 deg
-7E-05 -6E-05 -5E-05 -4E-05 -3E-05 -2E-05 -1E-05
SZ only
0.00015 -0.0001 -5E-05 0 5E-05 0.0001 0.00015
CMB + instr
-0.00015 -0.0001 -5E-05 0 5E-05 0.0001 0.00015
SZ + CMB + instr.
-0.00015 -0.0001 -5E-05 0 5E-05 0.0001 0.00015 0.0002
SZ + CMB + instr + submm

CLUSTER DETECTION

- Construct filter that enhances cluster signal whilst suppressing noise

- multi-frequency matched filtering uses knowledge of the spatial and spectral characteristics of cluster signal to *optimally* filter data

$$\Psi_{\theta_c}(\boldsymbol{k}) = \sigma^2_{\theta_c} \boldsymbol{P}^{-1}(\boldsymbol{k}) \cdot \boldsymbol{F}_{\theta_c}(\boldsymbol{k})$$

where

$$\boldsymbol{F}_{\theta_c}(\boldsymbol{k}) \equiv \boldsymbol{j}_\nu T_{\theta_c}(\boldsymbol{k})$$

$$\sigma_{\theta_c} \equiv \left[\int d^2k \, \boldsymbol{F}_{\theta_c}{}^t(\boldsymbol{k}) \cdot \boldsymbol{P}^{-1} \cdot \boldsymbol{F}_{\theta_c}(\boldsymbol{k})\right]^{-1/2}$$

c.f. Haehnelt & Tegmark 97,
Melin et al. 06

- filter data iterating over two β-models (β=2/3, 4/3) and gaussian, picking the template that provides highest S/N detection for each cluster

$$y(\boldsymbol{x}) = y_0(1 + |\boldsymbol{x}|^2/\theta_c^2)^{-(3\beta-1)/2}$$

Map Filtering

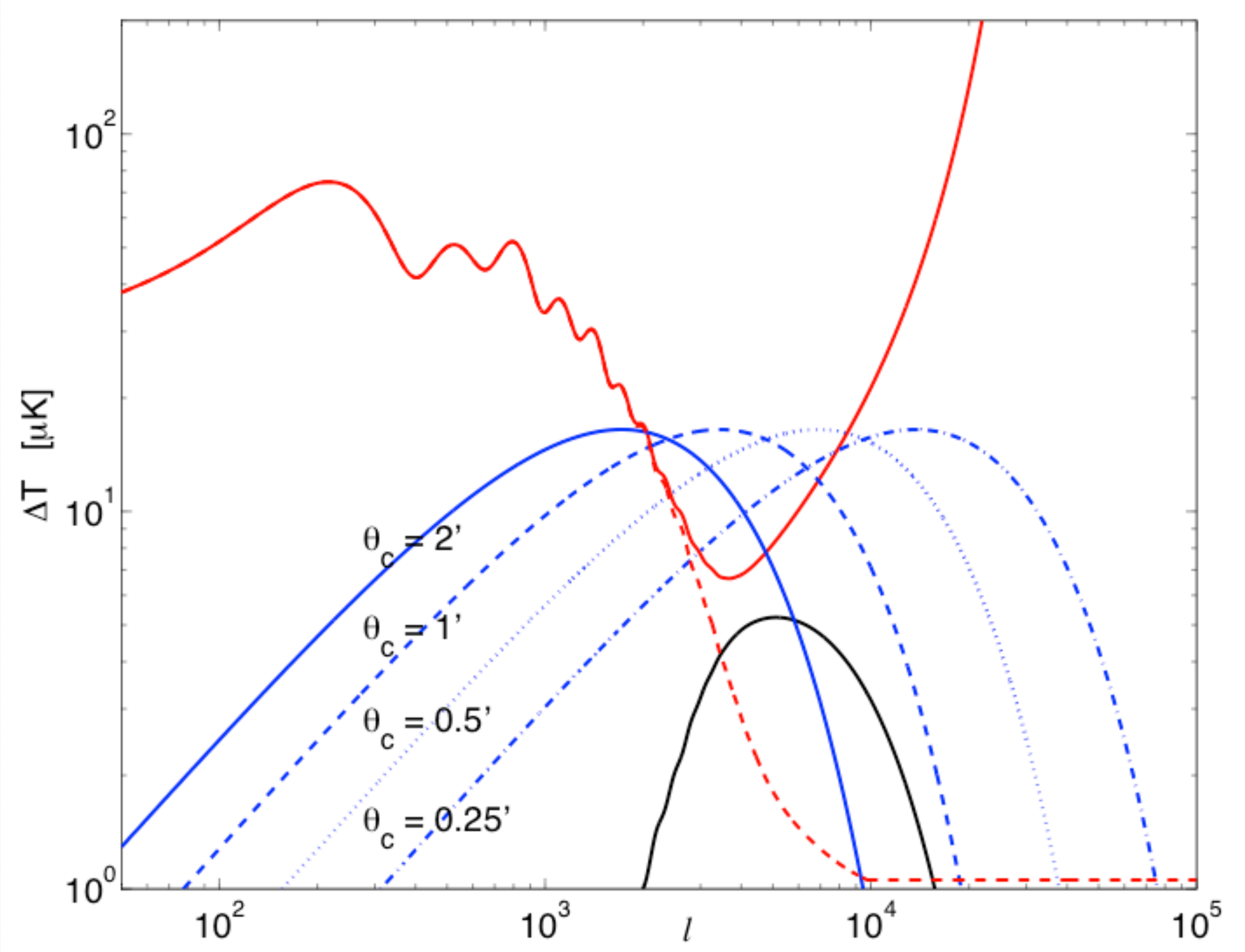

$$S_{\theta_c}(x) = y_0 \left(1 + \left(\frac{x}{\theta_c}\right)^2\right)^{-1/2} \longrightarrow 2\pi\theta_c \frac{\exp\left(-\theta_c l\right)}{l}$$

SZ only

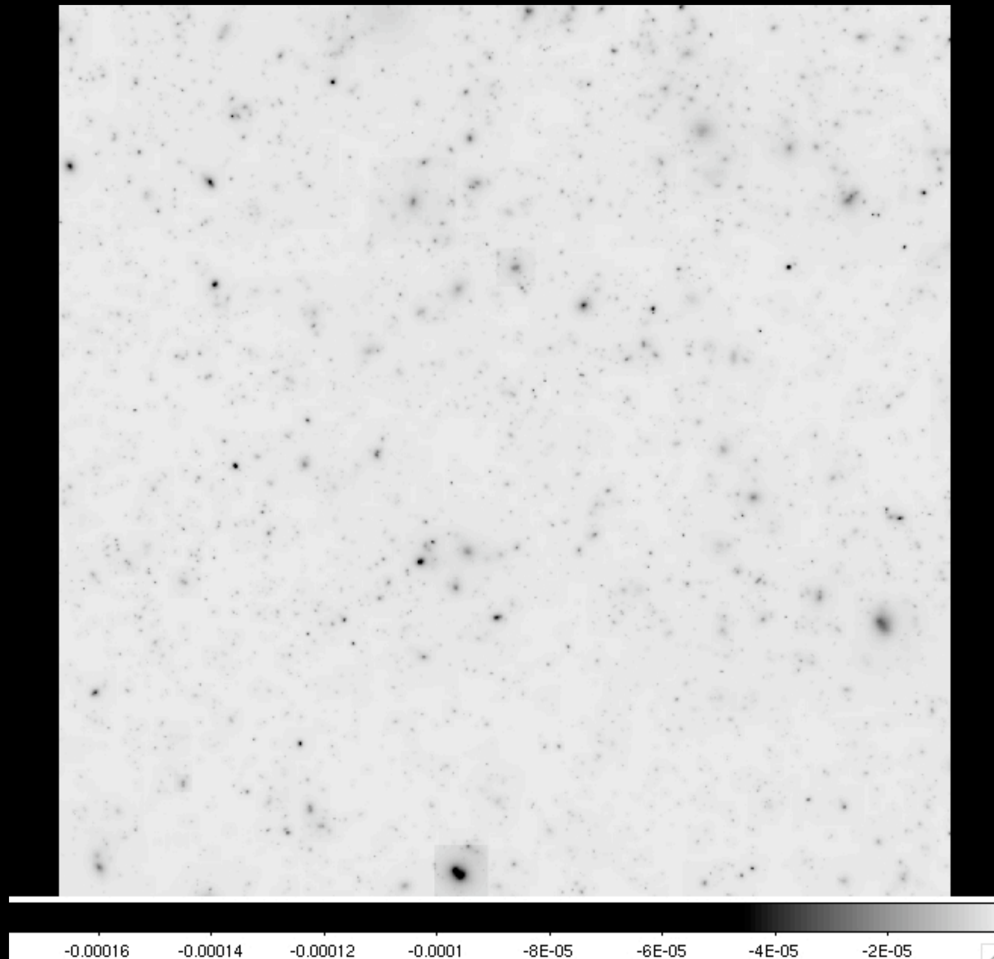

full map

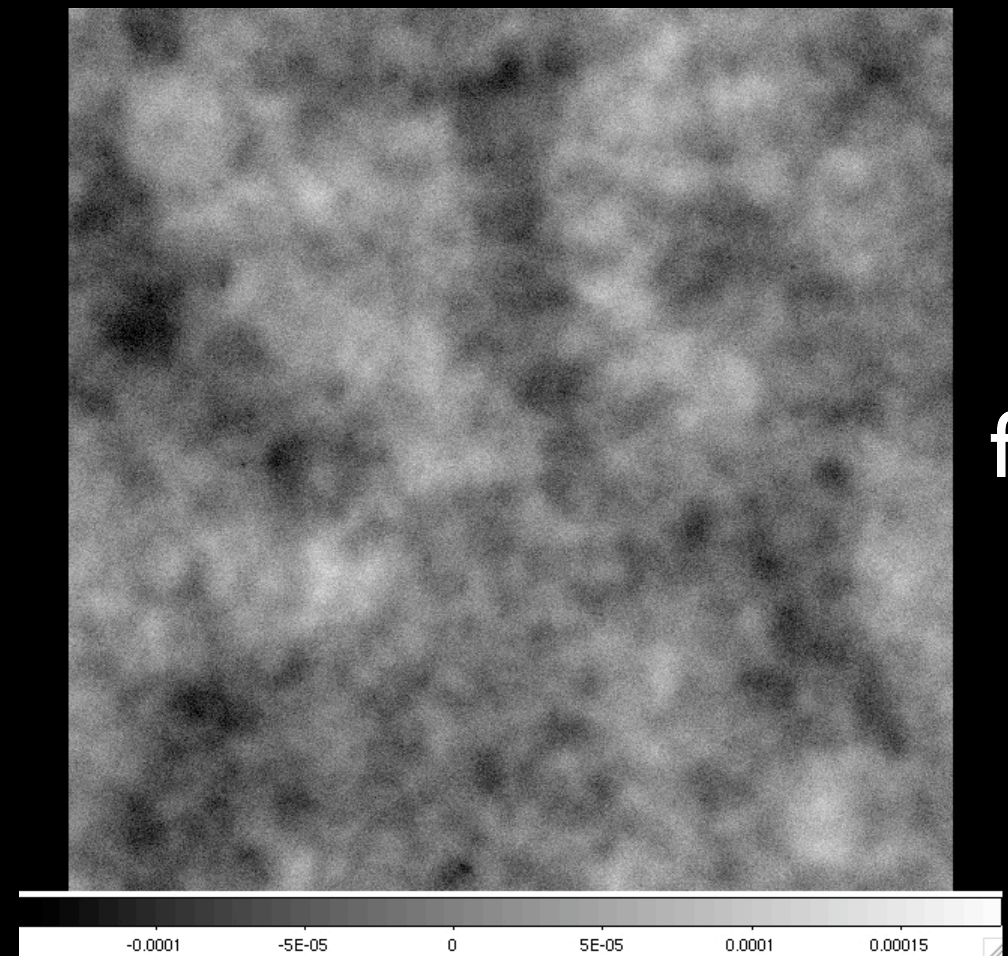

filtered
1 arcmin

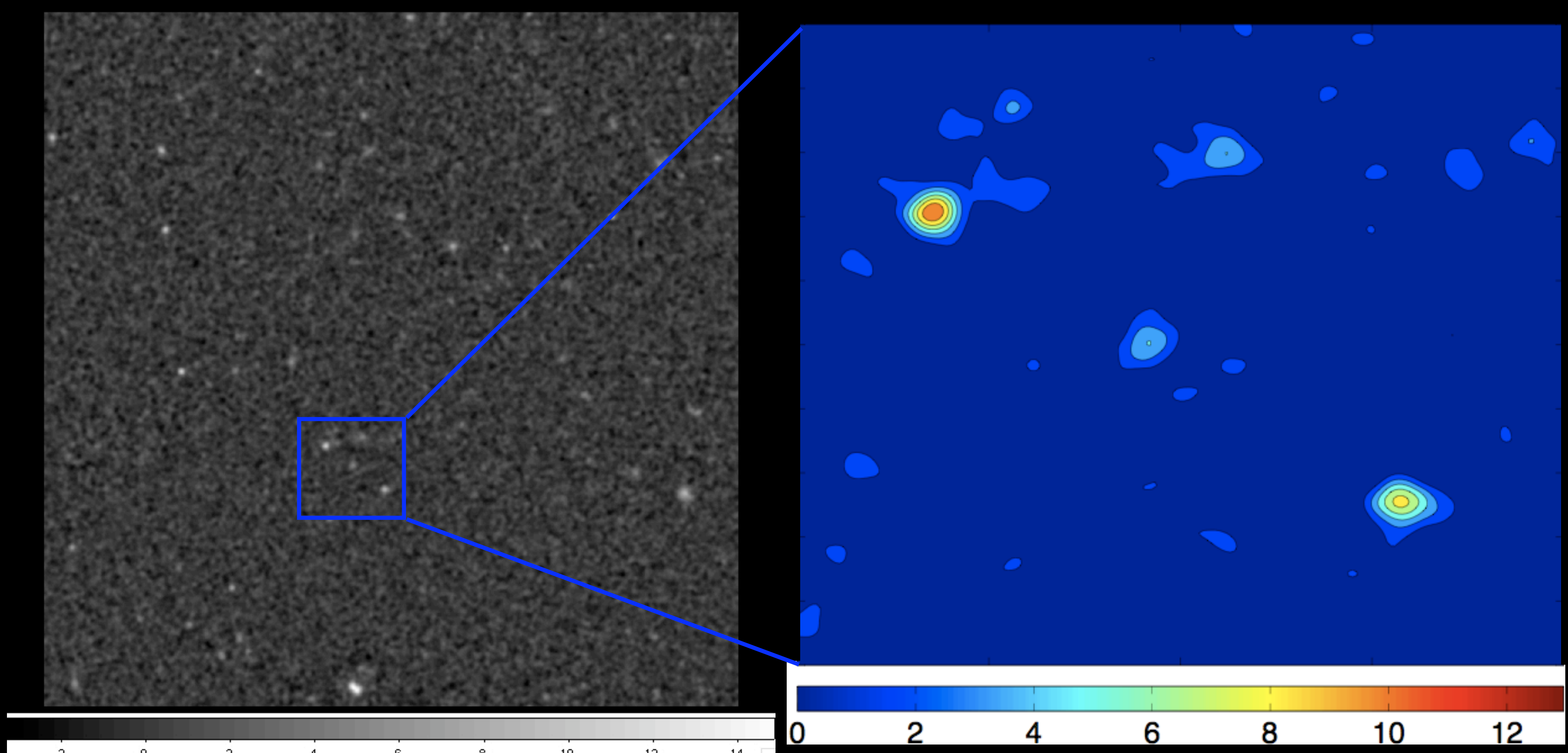

SURVEY CONFIGURATIONS

#	Noise [150 Ghz] μK arcmin^2 pixel	Noise [220 Ghz] arcmin^2 pixel	Area deg^2
1	7	19	100
2	14	40	500
3 a b	15 21	43 60	100 1000
4 a b	15 42	43 119	100 4000
5 a b	10 17	28 48	100 500

beam size [220,150] = [0.7',1']

	90Ghz	150Ghz	220Ghz	Area	beam [90,150,220]
3f	25	12.5	25	1000	[1.67',1',0.7']

FULL GAS MODEL YIELD

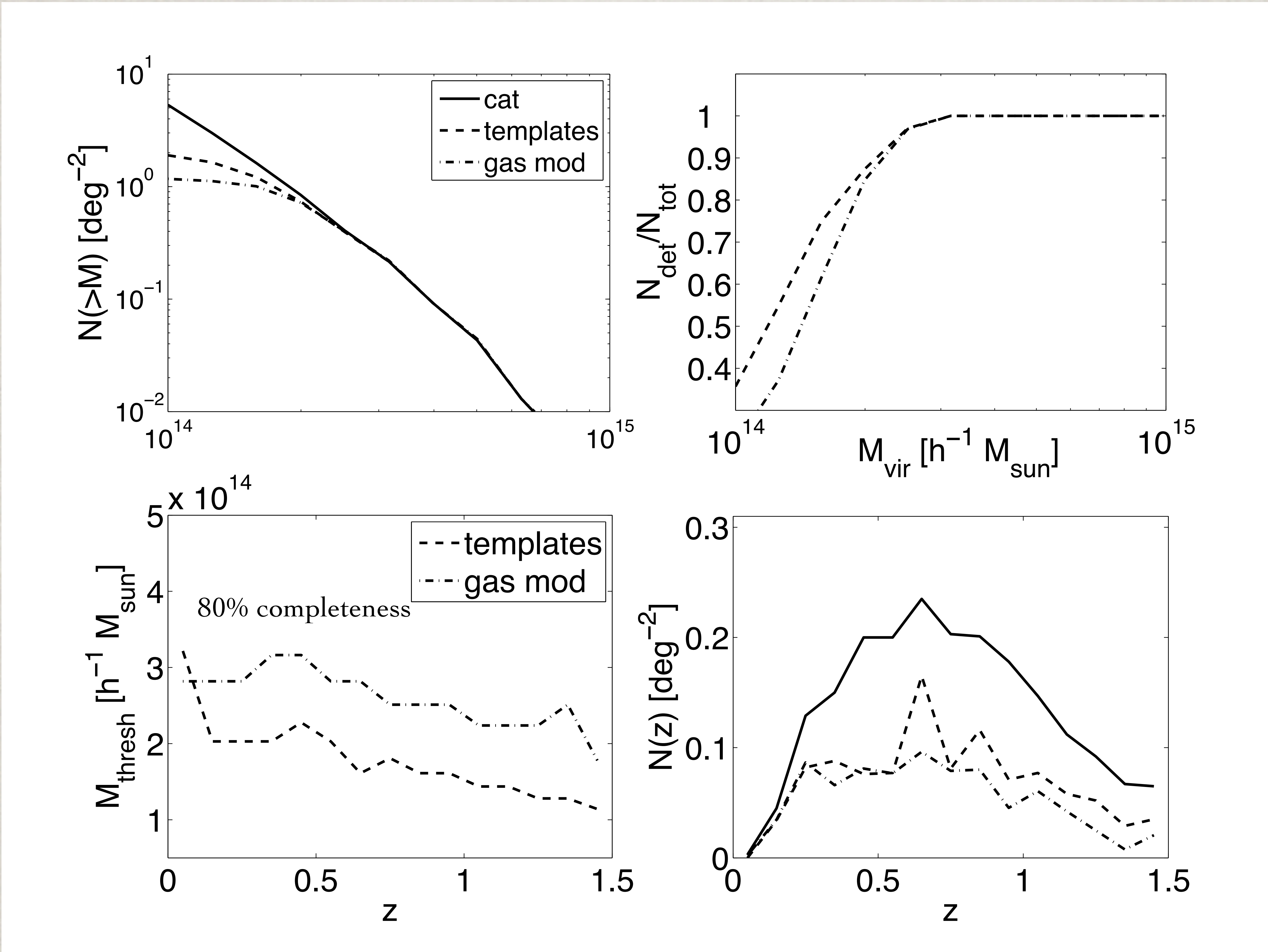

contamination < 10%

Dependence on profile

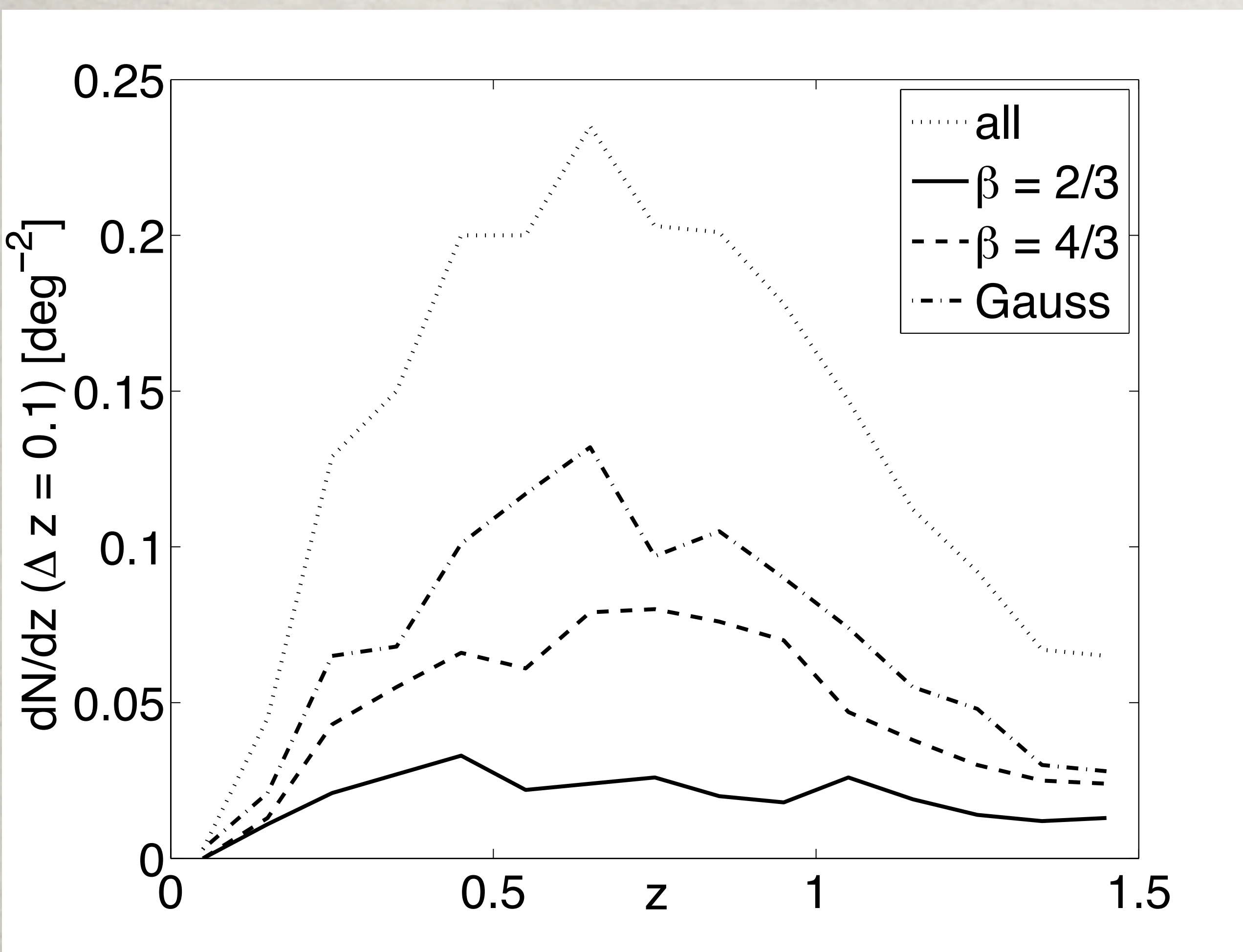

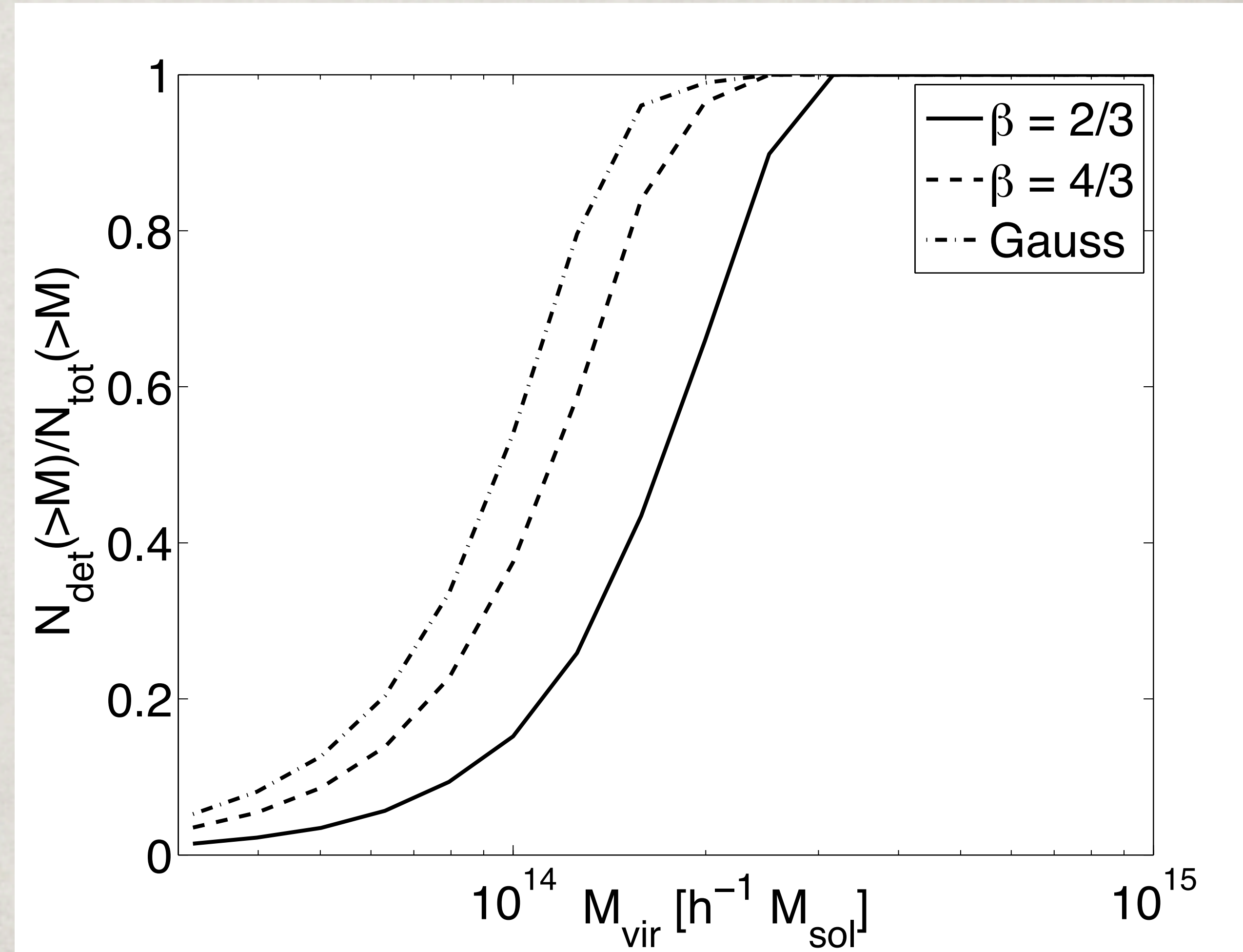

- Only 14% clusters selected had β=2/3 profiles, 50% had gaussian

$$y(\boldsymbol{x}) = y_0(1 + |\boldsymbol{x}|^2/\theta_c^2)^{-(3\beta-1)/2}$$

- 90% mass completeness at $1.5\text{x}10^{14}$ h^{-1} M_{sol} for gaussian, and at $2.5\text{x}10^{14}$ h^{-1} M_{sol} for β=2/3 profile

SURVEY YIELDS

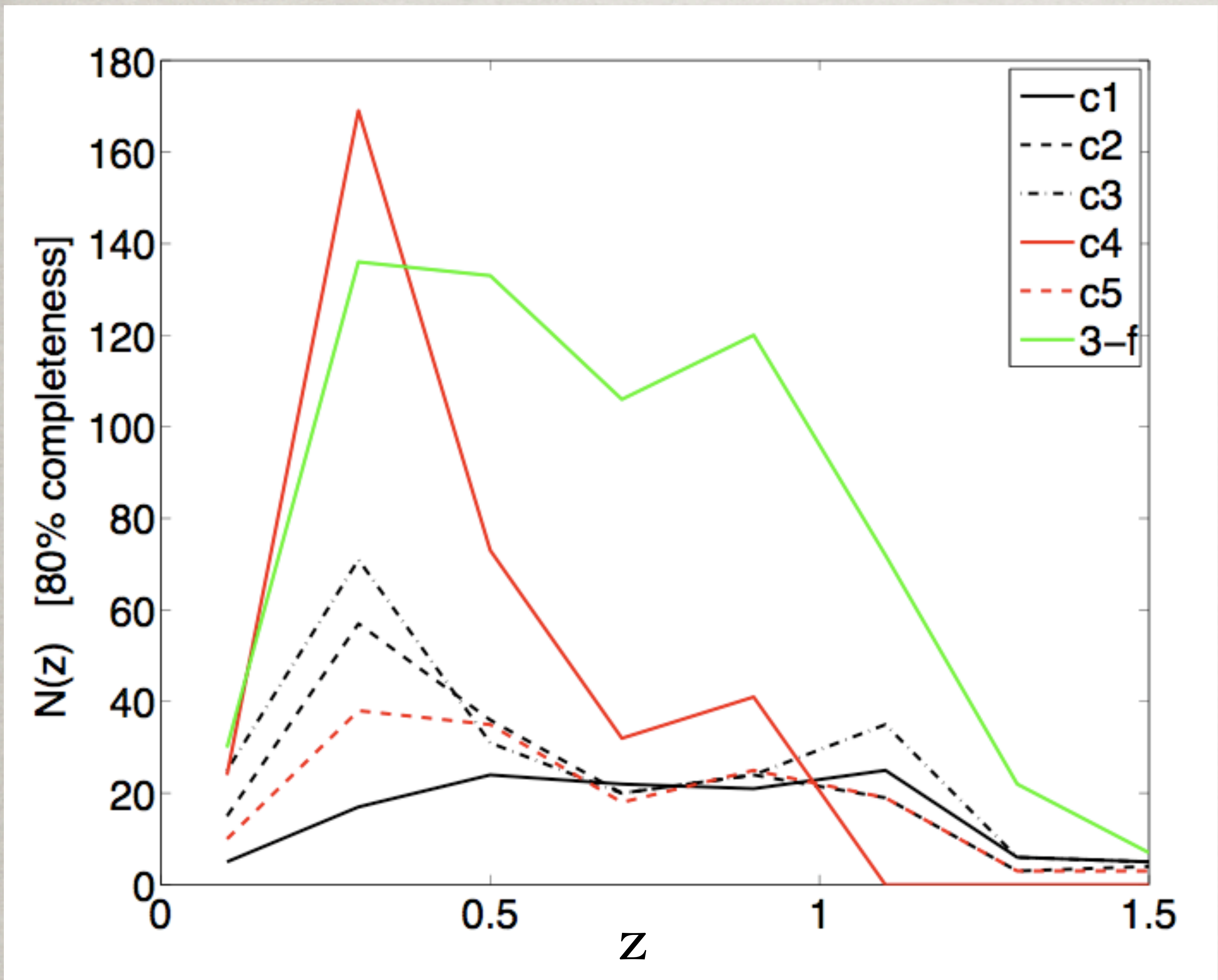

#	150Ghz	220Ghz	Area deg^2
1	7	19	100
2	14	40	500
3	15 21	43 60	100 1000
4	15 42	43 119	100 4000
5	10 17	28 48	100 500

	90	150	220	Area
3-f	25	12.5	25	1000

SURVEY YIELDS

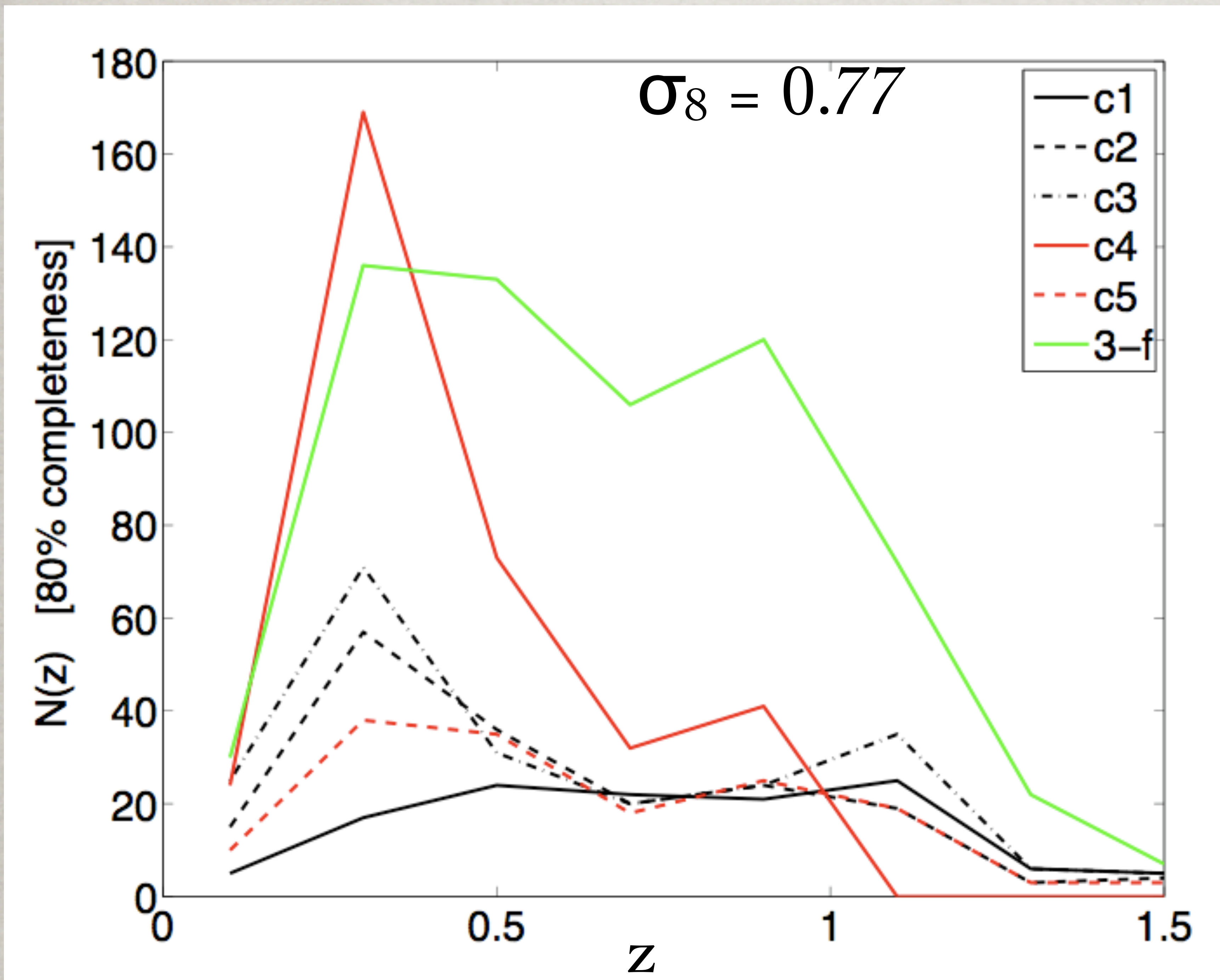

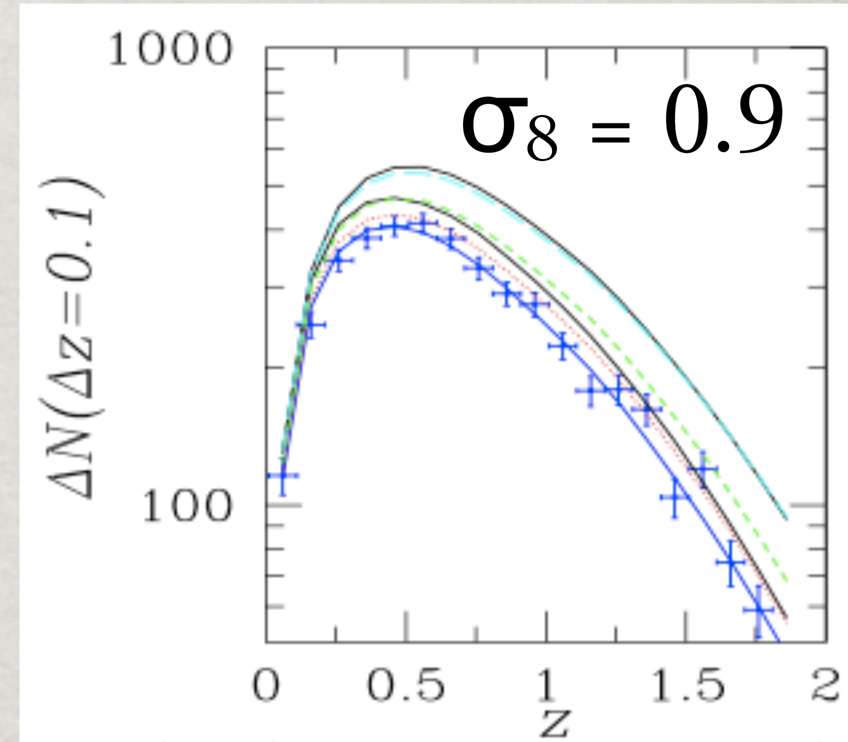

	21	60	1000
4	15 42	43 119	100 4000
5	10 17	28 48	100 500

	90	150	220	Area
3-f	25	12.5	25	1000

RECONSTRUCTING Y

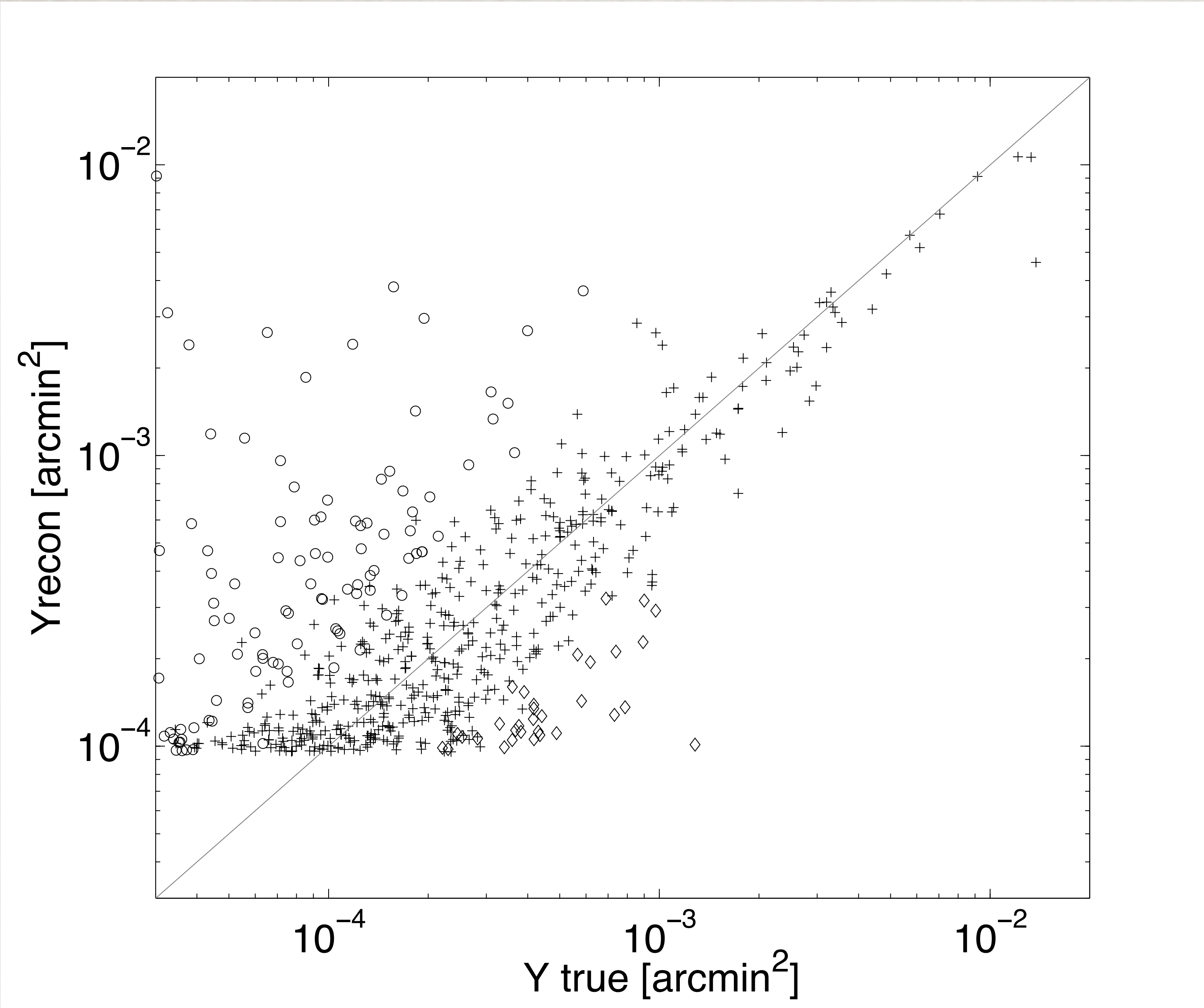

$$Y(\theta) = \int_0^{\theta} y(\theta) d\Omega$$

$$y_{obs}(\theta) = y_0 \left(1 + \left(\frac{x}{\theta_c}\right)^2\right)^{-1/2}$$

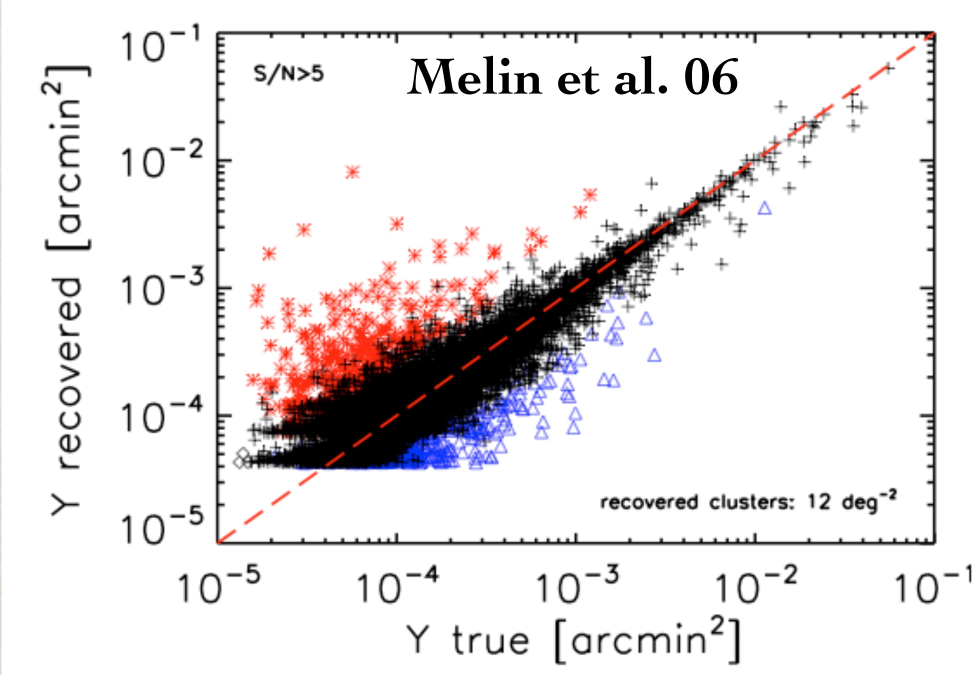

- Large scatter, even using β-model runs
- Error due to <u>poor estimation of core radius</u>, θ_c

ν	σ	beam
90	25	1.67
150	12.5	1
220	25	0.7

Impact of Beam

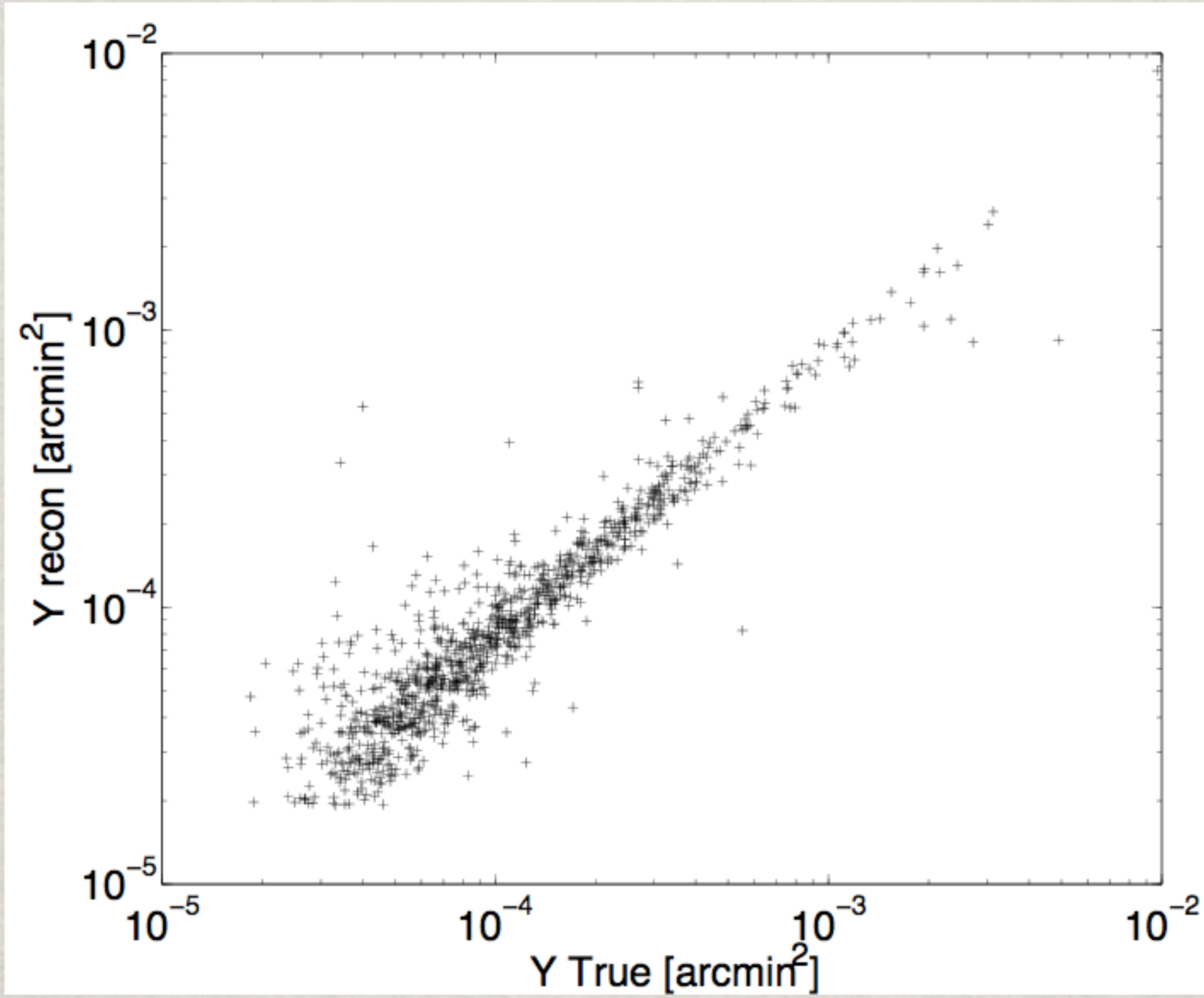

ν	σ	beam
90	25	0.17
150	12.5	0.1
220	25	0.07

- Survey synthetic maps with 1/10th beam size [0.17,0.1,0.07]
- Can measure cluster sizes with high degree of accuracy

USING S/N

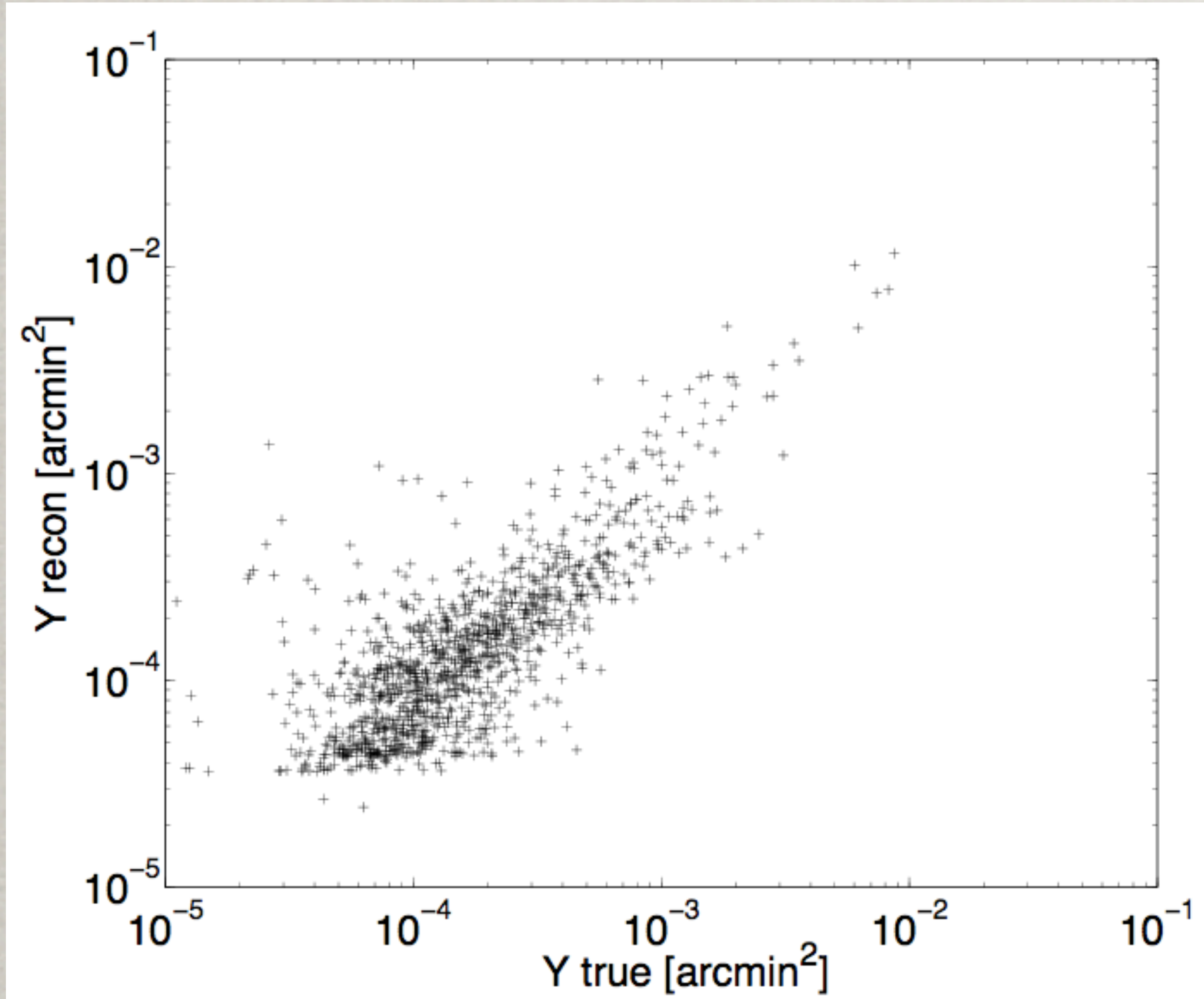

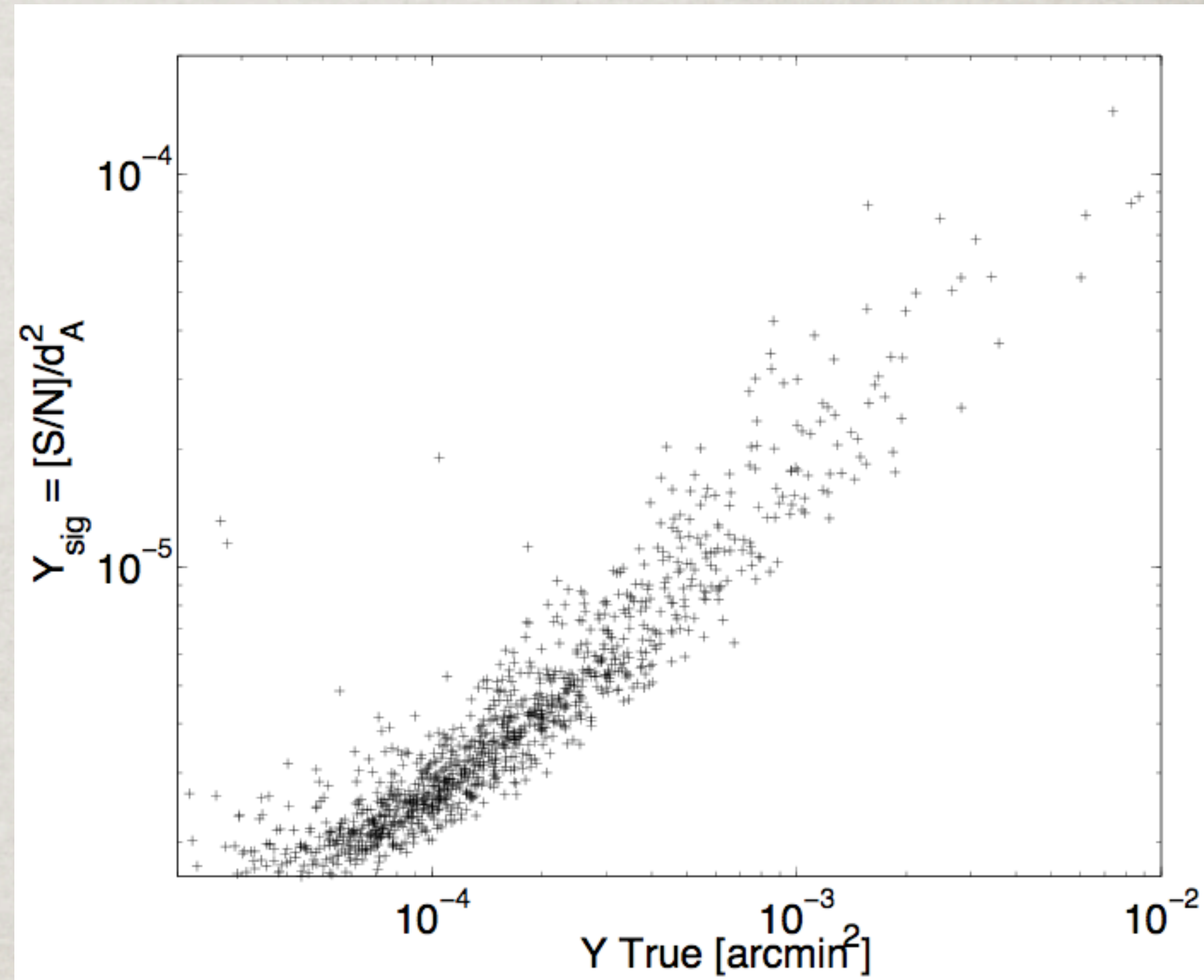

- Multi-template aids flux reconstruction
- Y_{sig} = [S/N]/d_A^2 appears to provide better Y measure

Parameter Estimation

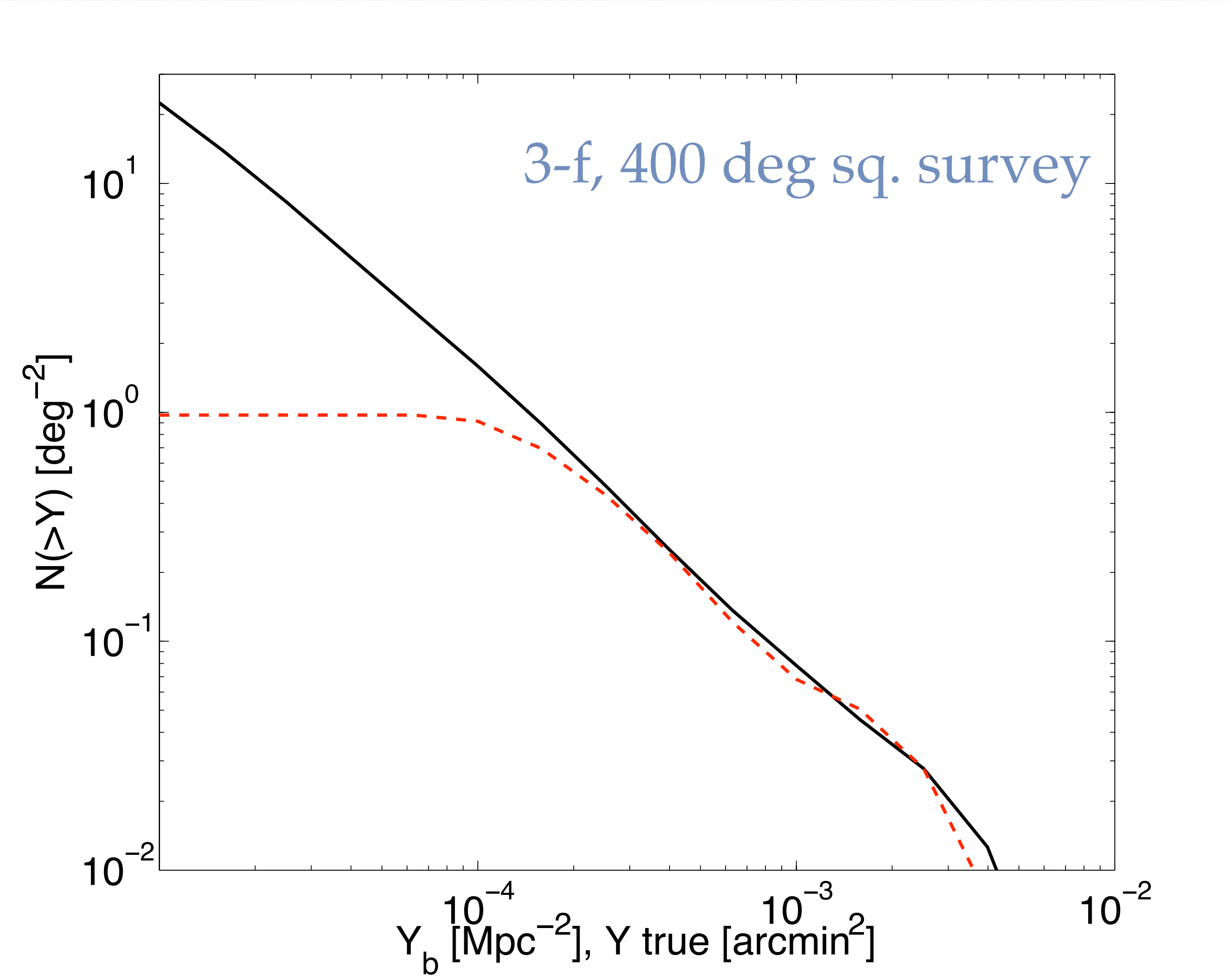

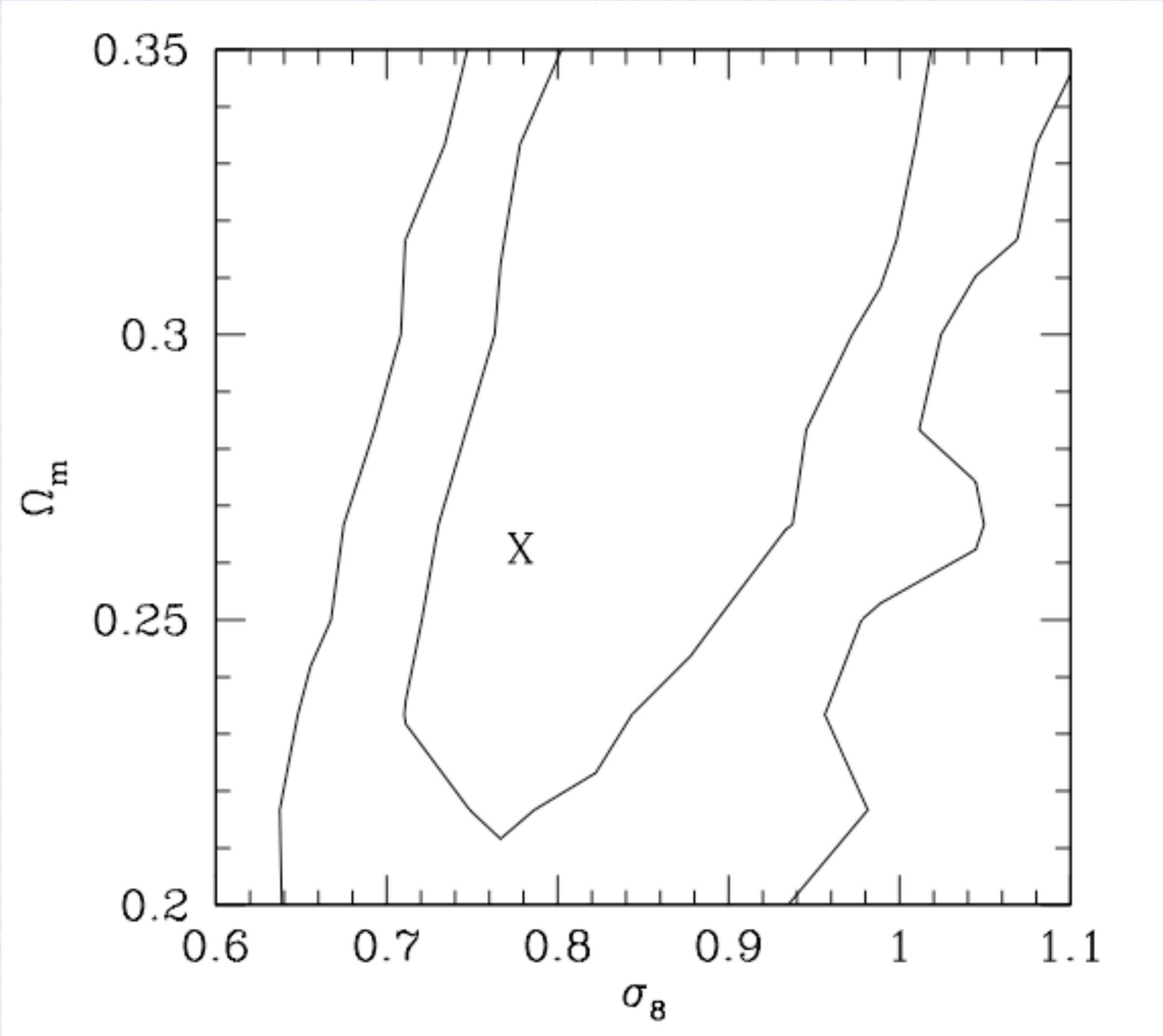

$$M_{obs} = A(z)e^{p(z)}$$

- Very important to understand cosmic evolution of s.r.

$$p(M_{obs}|M) = \frac{1}{\sqrt{2\pi\sigma^2_{\ln M}}} \exp\left[-x^2(M_{obs})\right]$$

$$x(M_{obs}) = \frac{\ln M_{obs} - \ln M - \ln M_{bias}}{\sigma_{\ln M}}$$

Multi-band Surveys

- To use N(z) to constrain cosmology need redshifts -> optical follow up / joint SZ + optical surveys
- SZ provides clean, flux-limited samples, wide z-range, but low S/N. Mostly limited to high-mass
- Optical
    - very large samples, high S/N gals
    - redshift-space distortions and projection effects produce catalogues with high contamination
- Conditional optical-SZ selection function
- Rate of mis-match, [see Cohn & White 08]

Optical - SZ cross matching

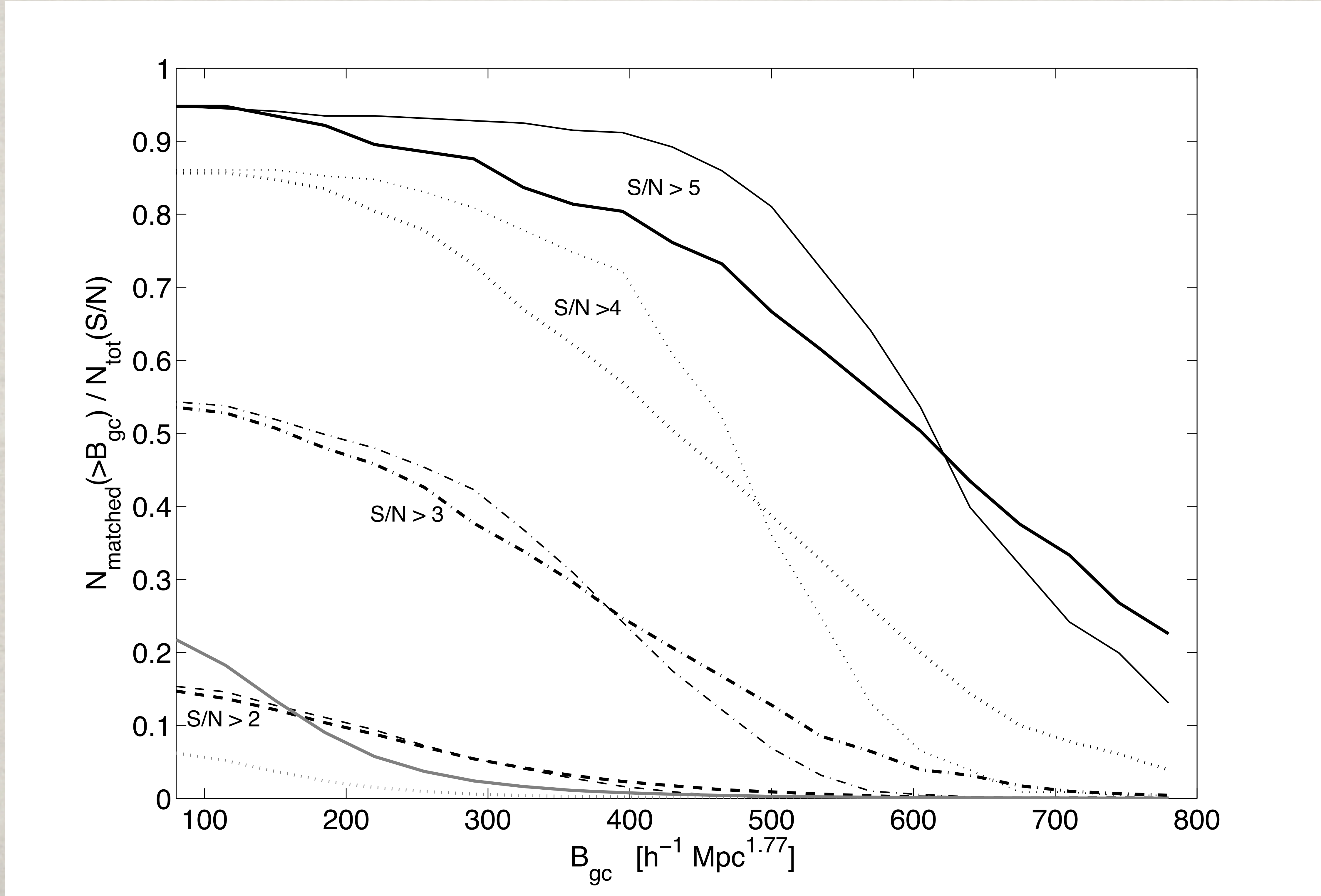

LENSING CALIBRATION OF Y-M

- stacked lensing signal should produce accurate estimates of halo mass
- Calibrate Y-M relation
- Break degeneracies between cluster + cosmological params. [Levine et al. 02, Mujumdar & Mohr 04]

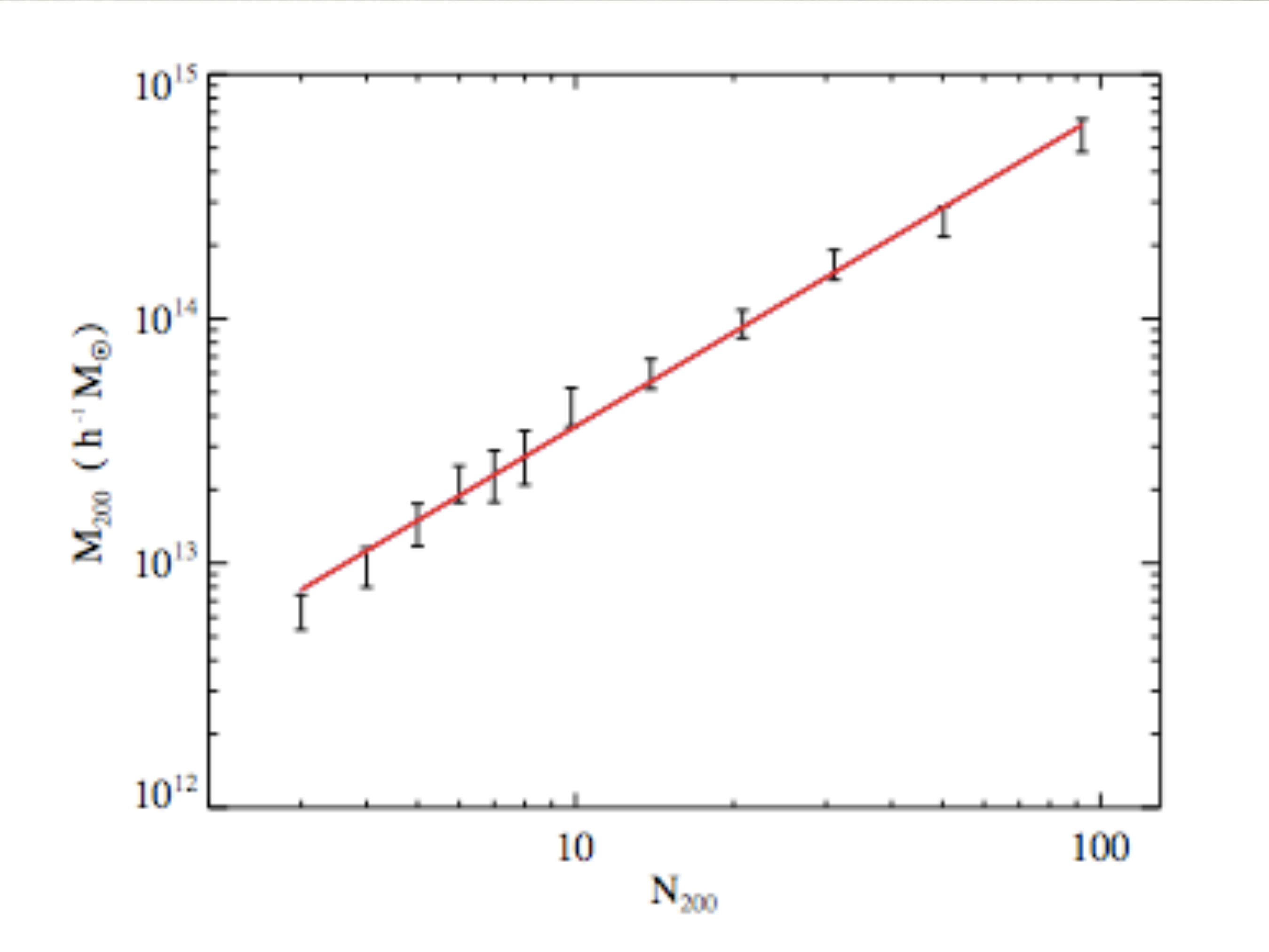

Johnston et al. (2007)

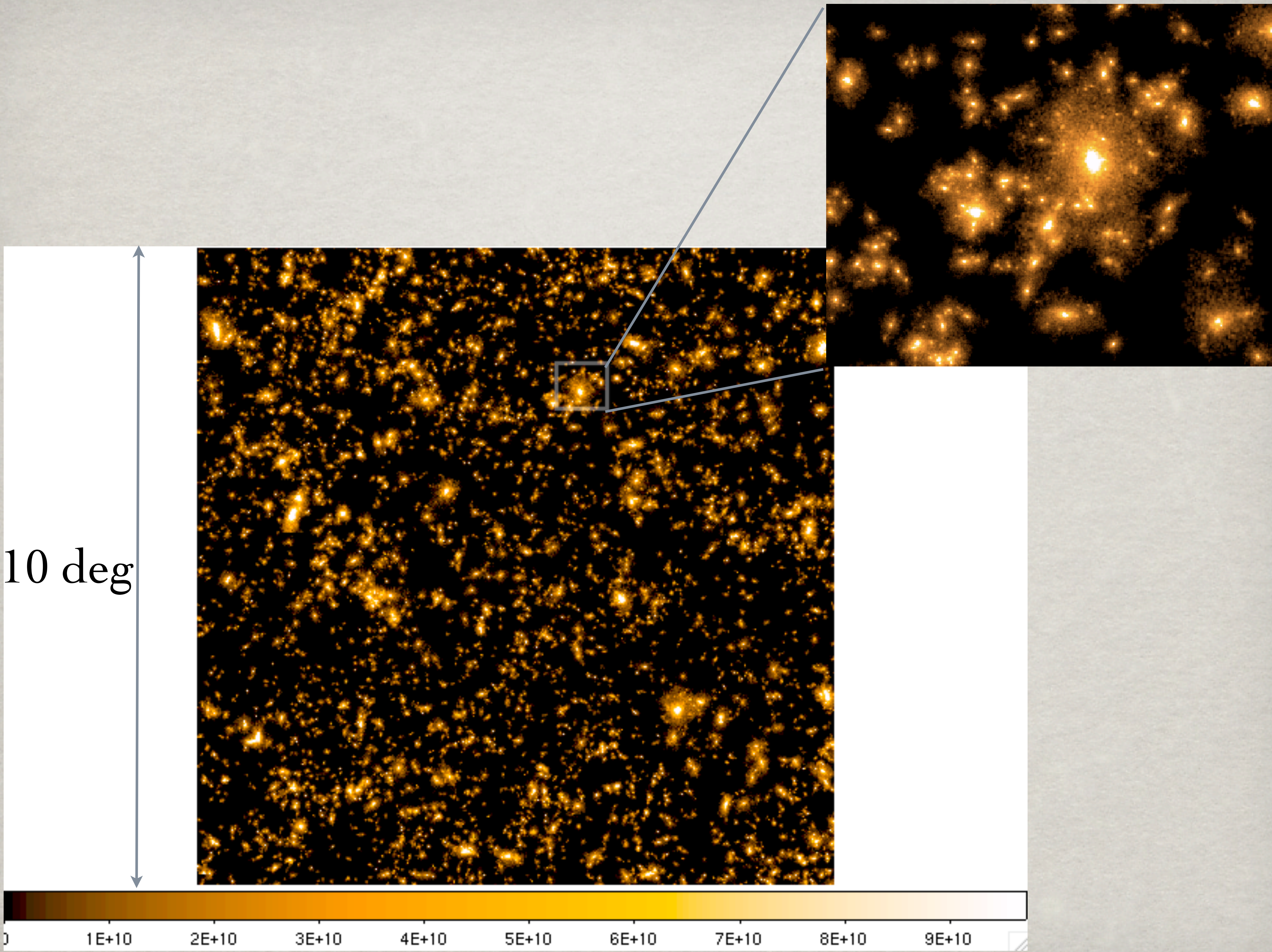
10 deg
0
1E+10
2E+10
3E+10
4E+10
5E+10
6E+10
7E+10
8E+10
9E+10

Conclusions

- Cluster number counts require good understanding of scaling of mass-obs relation, level of intrinsic scatter, cluster selection function, knowledge of sample completeness, purity
- Investigated scales at which SZ flux traces cluster mass e.g. Y ($<R_{500}$) correlates tightly with M_{200}
- Inclusion of non-gravitational energy in ICM significantly increases scatter in Y-M relation (driven by variation in f_b)
- variations in concentration can impact on gas dynamics and S.R. Substructure less so, but non-negligable.
- σ appears not to be normally distributed - form must be understood for self-calibration

- For $M < 2\times10^{14}\ h^{-1}\ M_{sol}$ SZ background significant l.o.s. contaminant. Measurements $Y(<1.5')$ should minimise impact of combined intrinsic + projection scatter w\ M.
- Have investigated cluster selection function for range of survey configurations. For fiducial strategy:
    - high completeness for $M > 2\times10^{14}\ h^{-1}\ M_{sol}$
    - <10% contamination
    - cluster profile impacts on S.F.
- Survey resolution strongly inhibits measurement of $y(\theta)$
- Other observables may correlate better (but need to be better understood)